Steam flows in concrete cracks: Design of an experiment

Jeremy Rabone, Christian La Borderie

Version of Record: https://www.sciencedirect.com/science/article/pii/S0029549322001613
Manuscript_bd9c3e536a533626820c7ef2b2e78de5

Steam flows in concrete cracks: design of an experiment

Abstract

An experimental setup to study nitrogen/steam mixtures flowing through cracks in concrete is presented. Mass flow regulators placed upstream of an evaporator allow the flow rate to be controlled precisely while thermocouples and pressure sensors placed near the entry and exit of the cracks accurately monitor the pressure and temperature fluctuations as the mixture flows. Thermocouples embedded just below the surfaces of the crack provide details of the temperature fluctuations within the crack, which indicate the formation of condensation and transfer of heat to the concrete.

Introduction

The function of the concrete containment structures of nuclear reactors is to act as barriers to the escape of radioactivity. The main function of an inner containment wall is to prevent the release of material in the case of failure of the primary pressurised containment. The inner containment wall of a reactor may include a metallic liner, but some reactors, notably some currently operating in France, use unlined concrete. A rupture in the primary circuit would leak steam leading to a rapid increase in pressure inside the containment structure at the same time as to a raised temperature and humidity inside. The concrete of unlined inner containment structures must therefore be able to withstand such abuse and maintain an effective barrier until the reactor is made safe.

Inner containment structures of working reactors are subject to decennial testing during which the internal pressure is raised and the subsequent evolution of the pressure is used to determine the permeability. Since these tests are carried out using air at ambient temperatures, there is some controversy as to how the resulting permeability should be interpreted in the context of containment of high-temperature steam. There is therefore an interest in determining relationships between the permeability of concrete structures to air and their permeability to high-temperature air-steam mixtures.

The presence of cracks in the concrete of an inner containment wall would obviously reduce its effectiveness as a barrier, but determining the rate at which material would be released through a given crack is a challenging problem (Caroli et al. 1995; Granger et al. 2001; Herrmann et al. 2016, 2017; Medjigbodo et al. 2016; Stegemann 2012). Following a rupture in the primary circuit, the mixture of heated air and steam within the inner containment is reckoned to reach up to 160°C and 6 bar absolute quickly, while the concrete of the containment wall is initially near ambient temperature. A quantitative model of the flow through a crack must therefore accurately treat the compressible flow of three phases (air, steam and water) and the heat transfer between them and the concrete (Bouhjiti et al. 2020; Jason and Masson, 2014; Nahas and Simon, 2005; Niklasch et al. 2005; Niklasch and Herrmann 2009; Rastiello et al. 2015a, 2015b; Simon et al. 2007; Zemann et al. 2019).

The latent heat of vaporisation of water around 120°C is about 2.2 kJ g^{-1} and the heat released by cooling water from 120°C to 20°C is about 400 J g^{-1}, while the heat released by cooling air from 120°C to 20°C is about 100 J g^{-1}. The steam, therefore, has the potential to heat the concrete far more than the air. The air, on the other hand, has a greater capacity to maintain the pressure within the crack as its volume only reduces by 25% on cooling from 120°C to 20°C, while water condenses with a volume

reduction of 99.99%. Condensation of the steam within the crack would lead to a local drop in pressure and heating while at the same time the higher viscosity of the condensed water (by roughly a factor of 40) would reduce the effective permeability of the crack. Localised reductions in pressure and heating would promote the evaporation of water, so raising the local pressure and cooling to local area. Meanwhile the transfer of heat to the concrete increases the temperature of the crack surface, reducing the surface temperature gradient and the rate of heat transfer to the concrete. Further complication arises from the absorption and/or release of water from the concrete and from the geometry of the crack itself.

The aim of this work was to devise and implement a test bench to control the experimental conditions as well as possible while monitoring the flow rate and temperature fluctuations within the crack in relation to these conditions.

The parameters requiring precise control are:

- Crack geometry,
- In-coming fluid temperature,
- In-coming fluid composition,
- In-coming fluid pressure,
- Initial concrete temperature,
- Initial degree of water saturation of the concrete,
- Outlet pressure.

For these experiments, nitrogen was used in lieu of air and the concrete was maintained in a water-saturated state by continual immersion between experiments. The biggest difficulty encountered during the design of the experiment was to control in-coming fluid temperature, pressure, flow rate and composition simultaneously and accurately. The compressibility of the mixture of nitrogen and steam demands that mass flow meters be used to obtain accurate flow rates. However, the facility with which the steam can condense requires that the flow meters and surrounding pipes be heated well above the temperature at which condensation could occur. The main problem with using heated flow meters was that the suitable flow meters available at the time the experiment was started were both very expensive and required recalibration each time the temperature and pressure regimes were changed significantly. An additional problem when mixing heated steam and nitrogen streams is to maintain a sufficient reservoir, or production of steam, in order to prevent the pressure upstream of the flow meter dropping too much as the steam flows, given that this either leads to a reduction in the steam temperature or to insufficient pressure. It was therefore decided that a better solution was to control the flow rate of cold nitrogen and water passing into an evaporator, and to monitor the in-coming fluid pressure[1].

Experimental details

1. Preparation and control of heated nitrogen steam mixtures

A schematic diagram and photograph of the apparatus used to generate heated mixtures of nitrogen and steam is shown in Figure 1.

[1] Flow meters are generally programmable and would allow a given pressure to be targeted by varying the flow rate, but rather than incorporate such variability it is preferable to operate the experiment with the flow rates fixed at appropriate values.

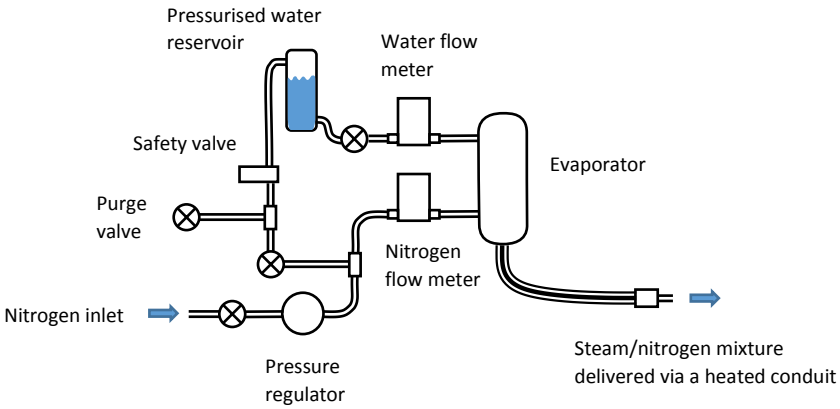

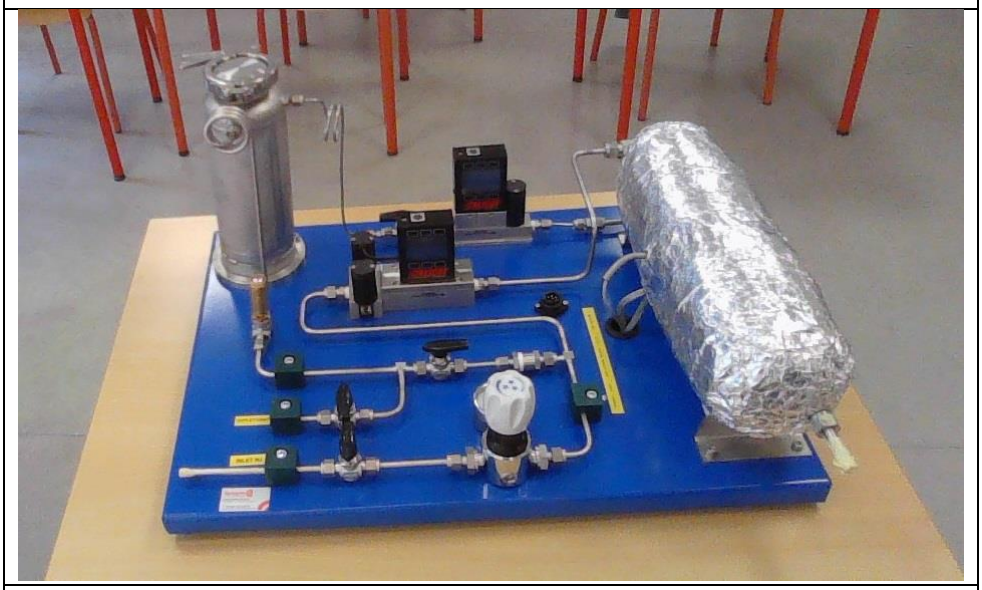

Figure 1: Schematic diagram and photograph of the heated steam/nitrogen mixture generator.

The generator employs two flow meters each with maximum capacities of 2 kg/hour to control the flows of nitrogen and liquid water, thereby allowing the overall flow rate and the proportion of steam to nitrogen in the mixture to be defined. The water flow meter (Alicat model LC-50CCM-D/5V) is actually a volume flow meter, but since the water is liquid, the conversion to mass flow is straightforward. For the nitrogen a mass flow meter is used (Alicat model MCH-50SLPM-D-PCV30/5M) in order to avoid errors in the flow rate that would arise from the compressibility of the nitrogen and the temperature/pressure variations. Each of the flow meters is connected to an interface cable that provides a measure of the flow rate as a voltage and could, in principle, be used to connect to a computer interface. In this setup, the flow rates are set manually via the flow meter control panels. The nitrogen is supplied from a bottle regulated at 6 bar and an integrated regulator controls the downstream pressure within the generator. The water reservoir is filled with deionised or distilled water and pressurised by opening a valve to the nitrogen line. A 6 bar safety valve is incorporated to prevent the water reservoir becoming over-pressurised and a purge valve allows the system to be depressurised. The outlets of the flow meters are fed into the evaporator, a heated vessel that heats and mixes the fluids with the power to generate up to about 1kg of steam per hour. The outlet of the evaporator is connected to a heated conduit that maintains the temperature of the

nitrogen/steam mixture as it is conducted to the sample. The temperatures of the evaporator and heated conduit are controlled by a pair of temperature regulators.

2. Preparation of model cracks in concrete

The MACENA project, of which these experiments are a part, resolved to use a single concrete formulation and mode of preparation across all laboratories and experiments in order to focus on the type of concrete typically used in reactor casings. Details of the formulation, preparation and the results of quality control tests conducted on samples of concrete prepared in the laboratory are given in the Supplementary Information A.

Cracks in concrete tend to follow fractal-like deviations roughly along a plane that is perpendicular to a tensional resultant stress within the concrete (Sun, 2011). The simplest model of a crack in the laboratory is therefore a rectangular channel with one dimension (the crack separation) considerably smaller than the other two. The focus of the initial experiments was to produce such model cracks of fixed width (2cm) and length (22cm) but varying separations. The method of preparation was developed with the intention of allowing the crack profile to be defined in later experiments using 3D printed inserts. This would allow the important effects of surface roughness and crack tortuosity on the flow to be investigated using the same apparatus.

The design of the model crack concept used in these experiments is drawn in figure 2. Two blocks of concrete (each 8cm wide, 22cm long and 6cm thick) are bolted together through aluminium tubes embedded in the concrete with round rubber joints retained by grooves in the concrete thus defining the sides of the rectangular channel. Steel spacers placed between the blocks ensure a minimum separation and high-temperature silicone (Silicoset 158) applied over concrete surfaces treated with epoxy resin ensures a good seal between the blocks.

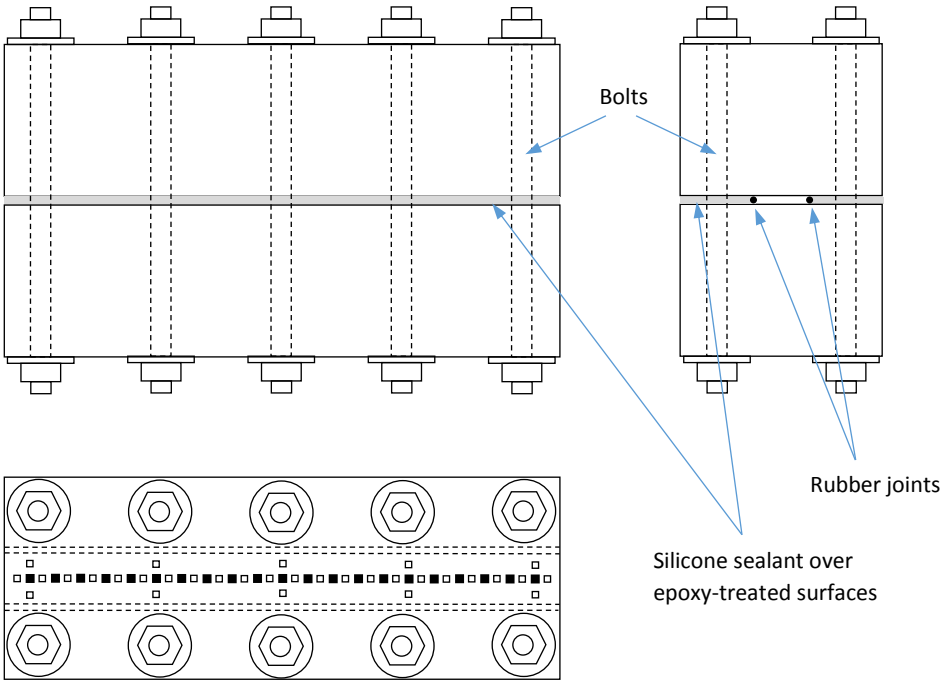

Figure 2: Design of the model crack concept showing side, top and front views. Thermocouples are embedded in the surface of the concrete above (filled squares) and below (open squares) the rectangular volume that is formed.

In order to monitor the temperature within the crack, it is necessary to embed thermocouples within the concrete in a manner that they are sensitive to the temperature within the crack while at the same time do not overly influence the thermal properties of the concrete. For these experiments, type-K thermocouples were used, and in order to minimise their influence on the conductivity of the concrete those used for embedding were twisted pair, fine wire models (200µm) with PFA insulation. To prevent the thermocouple junctions from contacting the fluid within the crack directly, while at the same time ensuring that the thermocouples were sensitive to the temperature of the fluid, small squares of mica about 75µm thick (cut from a transistor insulation plate) were used to form the interface between the junctions and the surface of the crack. Additional thermocouples embedded in the body of the concrete blocks could also be used to monitor their internal temperature. Further details of the preparation of the samples is given in the Supporting Information B.

3. Monitoring/controlling the experimental conditions

The heated mixtures of nitrogen and steam were passed through the model crack via stainless steel capsules that are clamped over the ends of the assembled blocks of concrete with a Viton rubber joint making the seal between the capsules and the block (Figure 3). The capsules each carry a thermocouple and a miniature high-temperature pressure sensor (TEI model PHT 861) which monitor the temperature and the pressure of the incoming and outgoing fluids. The pressure sensors were calibrated and compensated in the 20-175°C temperature range by the manufacturer but, owing to their high sensitivity, it was found necessary to apply an additional correction for a residual linear variation with the temperature. To this end, a thermocouple was taped to the casing of each pressure sensor in order to give reference temperatures for this correction (details in Supporting Information C).

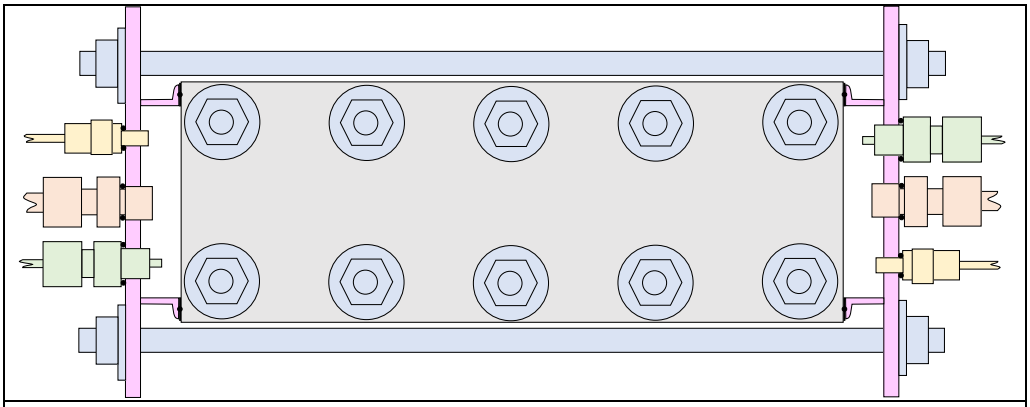

Figure 3: Diagram of the capsules assembled over a model crack. The concrete is shown in grey; the capsules in pink; stainless steel nuts, washers and bolts in pale blue; the Viton rubber seals in black; the pressure sensors in yellow; thermocouples in green and the inlet and outlet for the gas mixture in orange. The inlet is placed in the centre of the capsule while the outlet is placed toward the bottom to allow condensed water to drain freely.

The inlet capsule was heated with a 250W rope heater, controlled using a thermocouple taped to the outside of the capsule and a second thermocouple for safety. The heater was counter-coiled so as to

minimise the strength of the magnetic field it produces when the current flows (details in Supporting Information D). A sheet of mu-metal acted as a screen between the rope heater and the other components so as to further reduce the potential for interference. Fibre insulation (Superwool 607) was cut into shape and reinforced with aluminium tape in order to insulate the heated capsule thermally. A sheet of plastic was placed between the insulation and the concrete blocks to prevent humidity from reaching the heating coil since the concrete is initially wet and can otherwise cause an earth leakage fault on the electricity supply.

The tube from the outlet capsule can be attached to a back-pressure regulator setup comprising an Equilibar pressure regulator that is controlled through a second set-point regulator connected to the nitrogen bottle. The Equilibar permits the outlet pressure to be controlled accurately regardless of the flow rate and the mixture of gas, liquid and particles that could be released by the concrete. A trap could be attached to the exhaust tube to collect the condensed water before passing the rest of the gas through a tube filled with 4nm molecular sieve granules. By weighing the trap before and after an experiment it was possible to measure the amount of water that had passed through the crack.

Between experiments, the concrete was kept under water to ensure saturation of the concrete. Furthermore, during the experiments the exterior surfaces of the concrete were kept moist by spraying them with water. Since the initial temperature of the concrete is another important variable in the experiment, it is desirable to have a method to control it. It was initially envisaged to place the concrete and capsules inside a climate-controlled chamber, allowing them to reach equilibrium with the chamber temperature before commencing an experiment. For the initial experiments, an alternative heating method that was less cumbersome[2], albeit less well controlled, was to place two low-power PTC heaters (with a maximum surface temperature of 100°C) either side of the concrete and surround everything with more insulating blocks. A temperature regulator attached to a temperature sensor placed on top of the concrete controlled the target temperature. The low power of the heaters (about 10W each) evenly heated the concrete to a maximum temperature of about 55°C.

4. Conducting an experiment

The assembled concrete blocks are positioned between the capsules, the nuts of which are then tightened to a torque of 5 Nm. The insulation blocks are then placed around the heated entry capsule and the steam/nitrogen mixture generator is pressurised. The thermocouples, the pressure sensors and the flow meters are connected to an Agilent (Keysight) 34972A data logger via 34901A 20-channel multiplexers and recording is started. The temperature controllers of the evaporator, the heated conduit and the entry capsule are then set to the target temperature in increments of less than 60°C to avoid overshoot. After about 20 minutes of heating, the evaporator, heated conduit and entry capsule will have reached the target temperature and the air inside the entry capsule will be around 80°C[3]. The nitrogen flow rate is then set, followed by the water flow rate, and the pressures

[2] Assembling or dismantling the experiment in the climate-controlled chamber requires all of the thermocouples to be disconnected, disentangled and reconnected to the data logger, which takes about 3 hours.

[3] Since the air inside the capsule is also in contact with the wet concrete, it cannot reach the same temperature as that of the capsule without heating the concrete too much. Castem calculations were used to guide the design of the heating coil and the placement of the thermocouples in the absence of convection and evaporation, on the basis that this provided an upper limit to the temperatures that would be obtained.

registered on the flow meters are monitored to ensure that the pressures upstream are sufficient to maintain the flow[4].

The nitrogen/steam flows are maintained for 40-60 minutes, by which time the pressure differential will have stabilised and the established temperature gradients will be changing slowly. After this time, the flows are stopped, and the temperature controllers of the evaporator, heated conduit and entry capsule set back to 25°C. Data recording is continued for about 30 minutes, while the experiment starts to cool down. After this time, the recording is stopped and the model crack is removed and replaced under water. It is left in the water for at least 2 hours before attempting another experiment using it.

Exceptionally, experiments using flows of pure steam were conducted directly after an experiment using a flow of pure nitrogen, but having first allowed the pressure differential to drop to zero. The first and main reason for doing so is a more efficient use of time, since the pure nitrogen experiments reach steady state more quickly and transfer less heat to the concrete, with the conditions at the end of the experiment being practically the same as at the beginning. The second reason is that when an experiment is run with pure steam, it takes longer to dislodge the water already inside the crack and the steam condenses on the concrete. This leads to a series of erratic pressure oscillations at the beginning of the experiment which delay the onset of a steady state. The results of the pure steam experiments following a pure nitrogen experiment are practically the same as for a pure steam experiment starting from scratch, once the water initially in the crack has been cleared.

Results

The output of an experiment comprises the profiles over time of the mass flow rates, temperature and pressure readings from the inlet and outlet capsules, along with temperature readings of the pressure sensor casings, and temperature readings from the thermocouples embedded in the concrete. The sampling rate of the readings was generally set at the maximum of the data logger, which was about 46 milliseconds per reading, or about 2.7 seconds to sample all 59 readings of a sweep.

1. Examples of experiment outcomes

The graph in figure 4 shows the temperature and the pressure profiles typical of one of the experiments. After the initial warm up of the steam generator and the inlet capsule, the nitrogen and water flows are started and the pressure in the inlet capsule starts to rise. The inner surfaces of the model crack are heated as the hot fluid mixture flows through it, with sudden, smaller temperature fluctuations indicating steam condensation and the liberation of latent heat. Some of these condensation events are localised, indicated by a temperature peak that is registered by a single thermocouple, but the majority are concerted condensation events, indicated by peaks that are registered on several thermocouples at the same time.

[4] The flow meters require a pressure difference of about 1 bar between their inlets and outlets and as the pressure of the outlet approaches the pressure of the inlet, the flow rate drops and eventually stops.

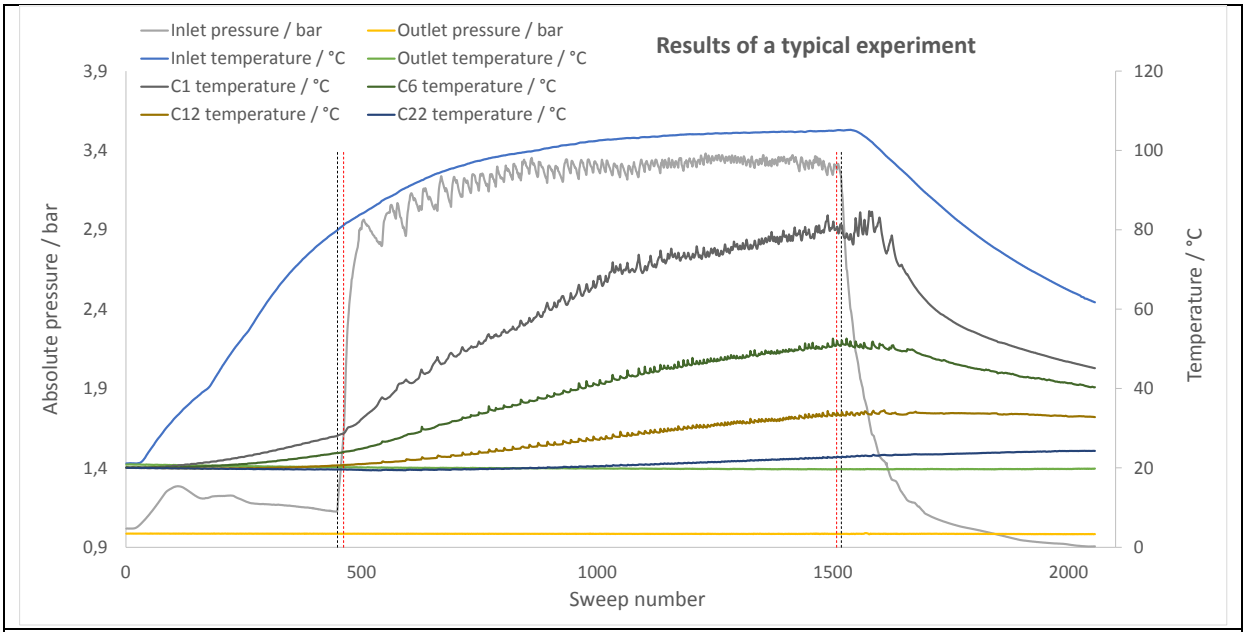

Figure 4: Results of a typical experiment showing the temperature profiles of 4 of the 43 thermocouples for clarity (C1 is 5mm from the crack inlet, C6 is 3cm from the crack inlet, C12 is 6cm from the crack inlet and C22 is 11 cm from the crack inlet and is the mid-point of the crack). The vertical black dashed lines mark the start and stop of the nitrogen flow, and the vertical red dashed lines the start and stop of the steam flow.

After a period of time (about 1100 sweeps or 50 minutes in the plot in figure 4), a quasi steady-state is attained where the pressure differential (the difference between the grey and yellow lines) is almost constant. The temperature of the concrete is steadily increasing as more heat is transferred from the heated fluid. When the water and nitrogen flows are stopped, the pressure drops while the steam generator depressurises through the crack. If there is any water that has condensed in the steam generator or the entry capsule, it may boil as the pressure drops and produces a sudden temperature increase (see the graph in figure 5). This is not a desired outcome of an experiment for it means that the steam has condensed before entering the crack because the inlet pressure rose above the vapour pressure of the water. The mixture entering the crack would initially have a reduced proportion of steam compared to the targeted mixture, and would be followed by liquid water once the level in the entry capsule reaches the crack.

In one of the experiments conducted on a sample with a crack separation of around 100µm, condensed water started to enter the crack half way through the experiment. Instead of the limiting behaviour of the typical pressure and temperature profile depicted in figure 4, a second increase in pressure occurred just as the pressure was starting to stabilise and was accompanied by temperature increases in both the entry and exit capsules as well as in all of the thermocouples (figure 5).

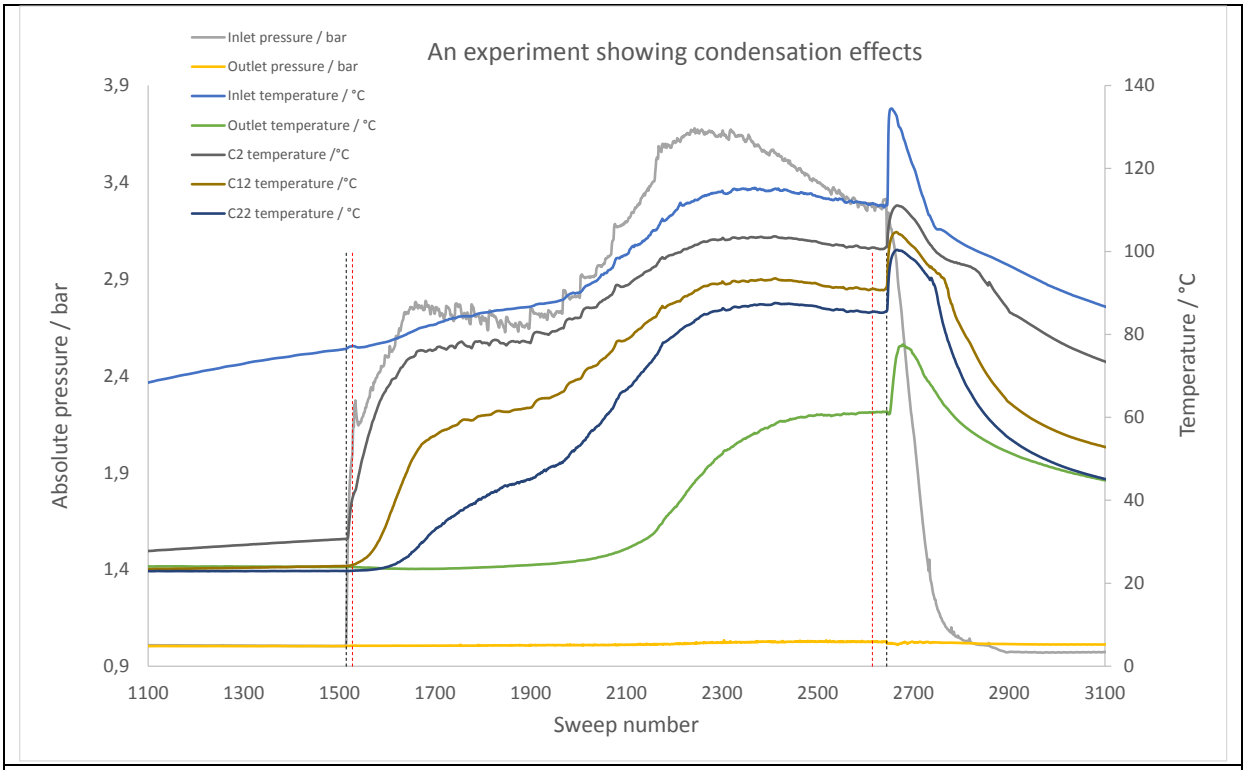

Figure 5: Result of an experiment where condensation in the steam generator and entry capsule has occurred. The fluid inlet temperature of this experiment was 120°C, at which the saturation vapour pressure of water is just under 2 bar absolute. Given that the pressure of the inlet rose above 2 bar, the fluid mixture produced in the generator would have contained both nitrogen, steam and liquid water. Once enough water had collected in the entry capsule (about 22 cm^3, equivalent to 350 sweeps in the graph above), it would have flowed into the crack, where the higher viscosity of the water would have caused the pressure in the entry capsule to rise further. When the pressure dropped after the nitrogen flow was stopped a little before sweep number 2700, the condensed water boils wherever it is above its boiling point, causing a sudden increase in temperature.

2. Effects of experiments on the samples

The first model crack prepared had, at first, an effective crack separation of 81 µm, determined from the pressure differentials established by flows of nitrogen at room temperature (see Supporting Information E). It was noted, however, that in the following experiments using the same model crack, the effective separation had reduced, as evidenced by an increased pressure differential for the same flow rate. Analyses of the pressure drops at the ends of each experiment (see Supporting Information E) gave values for the crack separation which indicate that the closing of the crack was linked to the number of experiments conducted with the model crack and not its age per se (Figure 6). Mineral deposits (Zemann et al. 2019) had formed on the inner surfaces of the model crack in response to the cycles of heating during experiments followed by re-immersion in water between experiments.

a)	b)

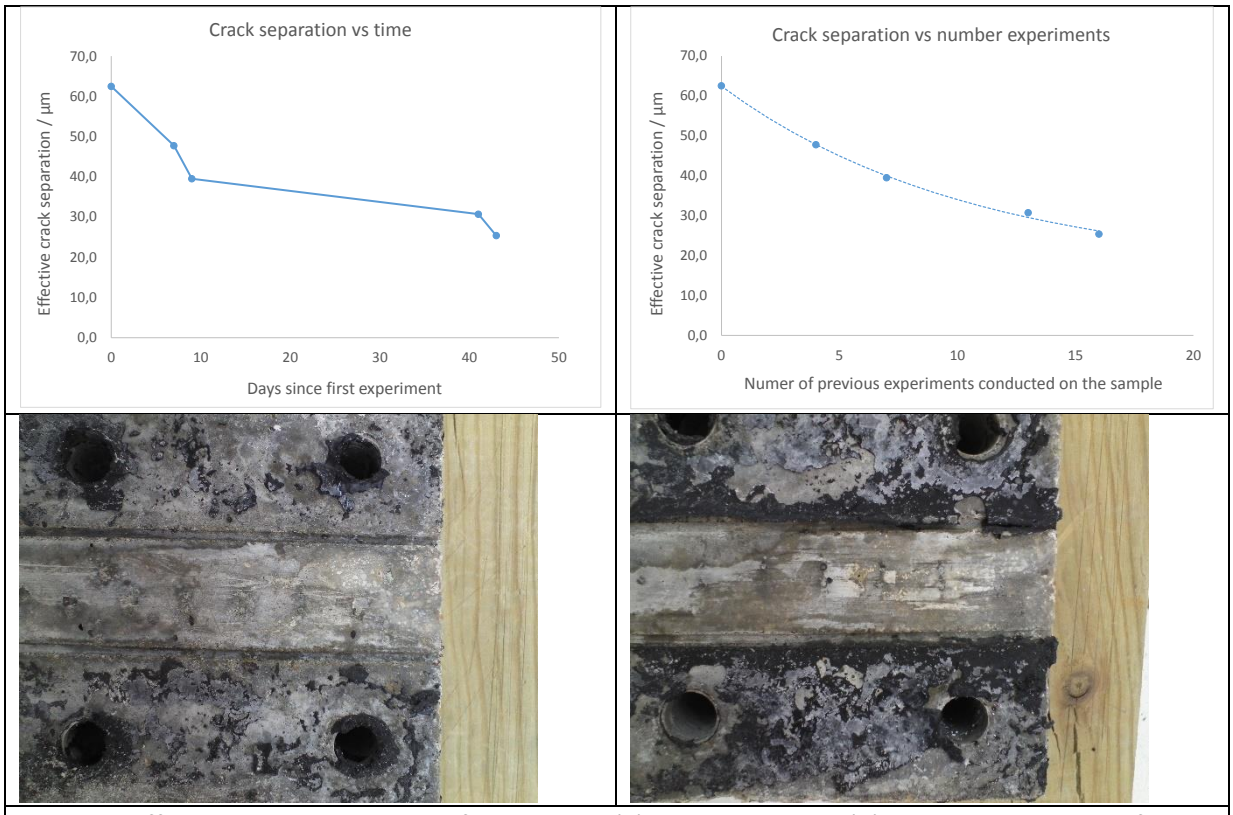

Figure 6: Effective crack separation of the sample (a) versus time and (b) versus the number of previous experiments conducted on the sample with a fitted exponential trend. The photographs show the mineral deposits on the model crack surfaces of the upper and lower blocks near the opening of the assembled model crack.

3. Variation of limiting pressure differentials with flow rate and steam content

For one model crack, the limiting pressure differentials for the experiments, taken as averages over the flat parts of the pressure trends, are plotted in figure 7. The graphs show the trends of the limiting pressures against gas mixtures, flow rates, fluid temperatures and the initial concrete temperature. The limiting pressures exhibit quadratic relationships both with the flow rates and with the proportion of steam in the mixture (the lines in the graphs of figure 7 are fitted quadratics). The theoretical limiting pressures shown in orange are those calculated from the average crack separations for each set of experiments, assuming that the concrete is at the same temperature as the fluid (see Supplementary Information F). The experimental values, shown in blue, are close to the theoretical values for the nitrogen portion of the mixture flowing at 20°C (not shown for clarity).

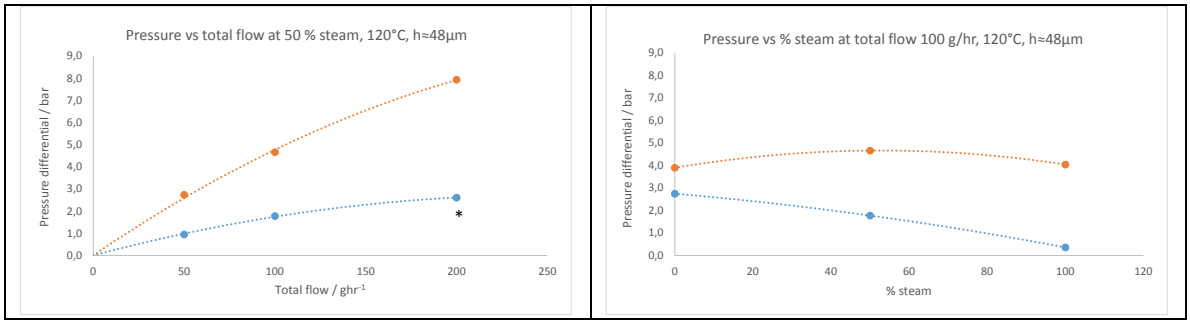

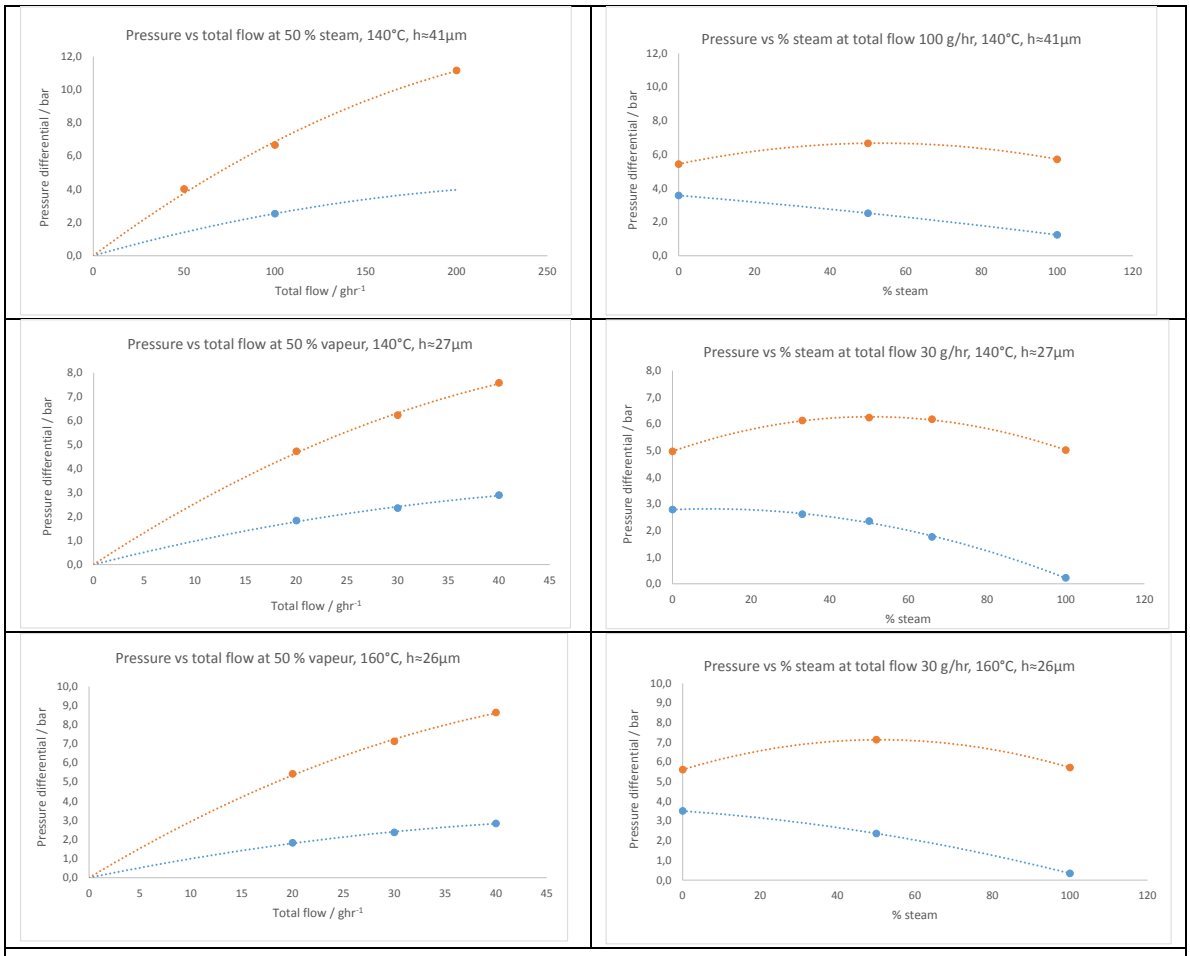

Figure 7: Trends of pressure differential vs total flow for mixtures of 50% steam by mass (left hand column) and of pressure differential vs %steam for fixed total flow (right hand column). The h values give the average crack separations for each set of experiments.

Comparisons between the trends are complicated by above noted variation in the effective crack separation between experiments. As well as using the results from experiments using pure nitrogen, one can also apply the same fitting procedure to the pressure drop curves from experiments with nitrogen/steam mixtures. In order for such a fit to be valid, any effects on the pressure caused by evaporation and condensation of water must be negligible, compared to those caused by the gas flow. This was found to be the case in experiments at low flow rates (i.e. small crack separation) in which all the steam had condensed as a result of cooling. It was not the case for experiments where significant quantities of water had condensed under pressure, given that the boiling of this superheated water when the pressure drops again interferes with the pressure drop.

4. Comparison of experimental and theoretical pressure differentials

Taking into account the crack separation obtained from each experiment, the limiting pressure that was measured can be compared with the theoretical limiting pressure at the temperature of the fluid. A graph showing the ratios for this set of experiments is shown in figure 8. The curve produced by the experiments at 140°C and a crack separation of around 27µm has a characteristic shape. This shape can be explained by the ratios of the theoretical limiting pressures of the nitrogen/steam

mixtures when the concrete is also at the same temperature, and the theoretical limiting pressure of the pure nitrogen component at 20°C (see Supporting Information F).

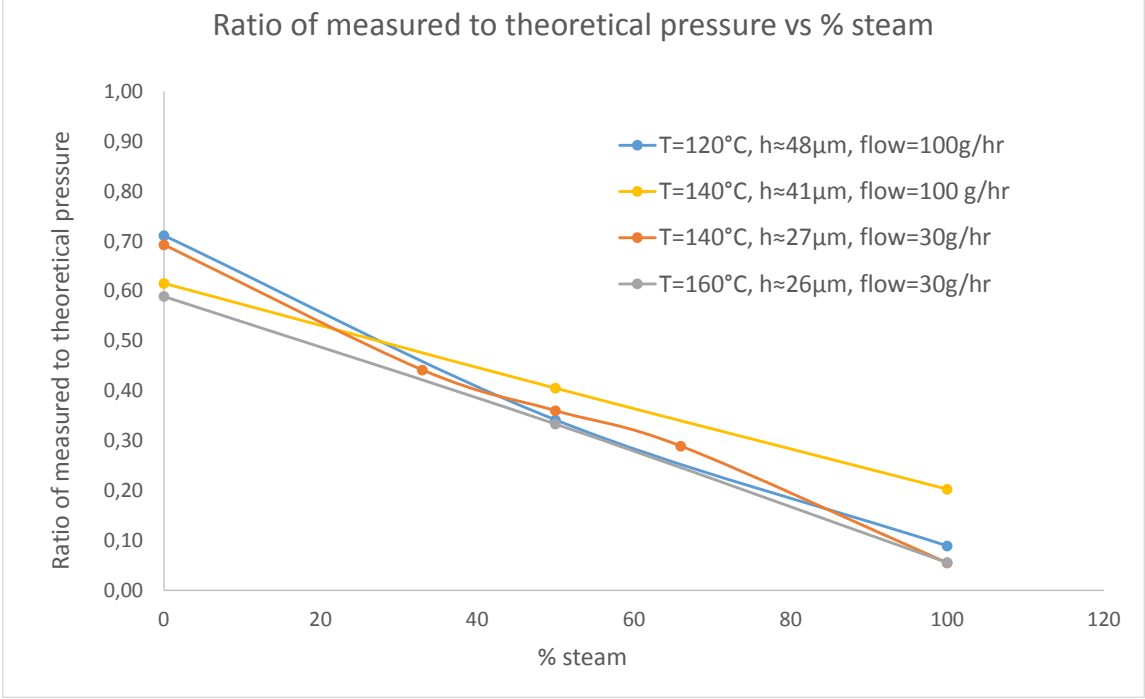

Figure 8: Ratios of measured limiting pressure to the theoretical limiting pressure when the concrete is at the same temperature as the fluid, plotted against the % of steam.

Conclusions

The validity of an experiment to pass well-characterised flows of nitrogen/ steam mixtures at temperatures between 100°C at 160°C and pressures up to 6 bar absolute through model cracks has been demonstrated. Mass flow controllers combined with a heater/mixer allow accurately measured flow rates of nitrogen and steam to be delivered to samples via a heated conduit. Capsules carrying pressure sensors and thermocouples clamped over the ends of the samples provide measures of the pressure and the temperature of the fluid in the capsules. By heating the inlet capsule to the same temperature as the steam generator, the temperature of the flowing mixture is maintained up to the sample.

A method to produce model cracks in concrete with accurately-placed thermocouples along the surfaces of the crack has been introduced. By casting the thermocouples into concrete blocks which can be subsequently bolted together with spacers and suitable seals, it is possible to produce a range of crack separations. Mineral deposits were found to form on the inner surfaces of the cracks in response to the heating during the experiments and caused a corresponding reduction in the crack separation.

The series of experiments conducted on this sample have demonstrated non-linear relationships between the mass flow rate and limiting pressure on the one hand, and the proportion of steam in the mixture and the limiting pressure on the other. Comparison with the theoretical limiting pressure calculated as if the concrete was at the sample temperature as the mixture, has demonstrated an increasing difference between the two values with increasing flow rate and increasing proportion of

steam in the mixture. The ratios of the two sets of values versus the proportion of steam in the mixture all fall close to a line that indicates that the nitrogen/steam mixture is effectively cooled to the same temperature as the concrete. The observable effect of this is that the pressure differential drops for a constant mass flux with increasing proportion of steam[5].

Temperature fluctuations have been measured by the thermocouples and found to be linked to the condensation of steam within the crack[6]. Associated pressure fluctuations have been observed in the pressure sensors.

Acknowledgements

Laurent Marlin and his team at the University of Pau are acknowledged for their fine work in the fabrication of the capsules. SystemC Instrumentation are acknowledged for their kind help with the design and assembly of the steam generator.

This work was funded by the Agence Nationale de la Recherche (ANR) as part of the MACENA project (ANR reference 11-RSNR-0012). We would like to thank the project partners at Electricité de France (EDF), Institut de Méchanique et d'Ingenierie Bordeaux (I2M) and the laboratoire Sols, Structures Solides, Risques (3SR) Grenoble for their amiable collaboration.

References

Bouhjiti, D.E.-M., Baroth, J., Dufour, F., Michel-Ponnelle, S., Masson, B., 2020. Stochastic finite elements analysis of large concrete structures' serviceability under thermo-hydro-mechanical loads – Case of nuclear containment buildings. Nuclear Engineering and Design, Volume 370, 110800. https://doi.org/10.1016/j.nucengdes.2020.110800

Caroli, C., Coulon, N., Renson, C., 1995. Steam leakage through concrete cracks: parametric study with SIMIBE experiment and interpretation of the results. Technical Report of the Commissariat à L'Energie Atomique (CEA).

Granger L., Rieg C.Y., Touret J.P., Fleury F., Nahas G., Danisch R., Brusa L., Millard A., Laborderie C., Ulm F., Contri P., Schimmelpfennig K., Barre F., Firnhaber M., Gauvain J, Coulon N., Dutton L.M.C., Tuson A., 2001. Containment Evaluation under Severe Accidents (CESA): synthesis of the predictive calculations and analysis of the first experimental results obtained on the Civaux mock-up. Nuclear Engineering and Design, Volume 209, Issues 1-3, Pages 155-163.

Herrmann, N., Müller, H.S., Michel-Ponnelle, S., Masson, B., Herve, M., 2017. The PACE-1450 Experiment - Investigations regarding crack and leakage behaviour of a pre-stressed concrete containment. High Tech Concrete: Where Technology and Engineering Meet, Pages 1487-1495. https://doi.org/10.1007/978-3-319-59471-2_171

[5] The relationships between the steam content, mass fluxes and pressure differentials for different crack separations will be the subject of a future publication.

[6] A detailed analysis of these temperature fluctuations will be the subject of a future publication.

Herrmann, N., Müller, H.S., Niklasch, C., Michel-Ponnelle, S., Masson, B., 2016. The PACE-1450 test campaign - Leakage behaviour of a pre-stressed concrete containment wall segment. Key Engineering Materials, Volume 711, Pages 863-870. https://doi.org/10.4028/www.scientific.net/KEM.711.863

Jason L., Masson B., 2014. Comparison between continuous and localized methods to evaluate the flow rate through containment concrete structures. Nuclear Engineering and Design, Volume 277, Pages 146-153. https://doi.org/10.1016/j.nucengdes.2014.06.010

Medjigbodo S. M., Choinska M., Regoin J.-P., Loukili A., Abdelhafid K., 2016. Experimental study of the air–steam mixture leakage rate through damaged and partially saturated concrete. Materials and Structures, Volume 49, Pages 843-855. https://doi.org/10.1617/s11527-015-0542-5

Nahas G., Simon H., 2005. Air-steam leakage through cracks in concrete. Nureth 11, eleventh international topical meeting on nuclear reactor thermal hydraulics, France.

Niklasch C., Coudert L., Heinfling G., Hervouet C., Masson B., Herrmann N., Stempniewski L., 2005. Numerical investigation of the leakage behaviour of reinforced concrete walls. Nureth 11, eleventh international topical meeting on nuclear reactor thermal hydraulics, France.

Niklasch, C., Herrmann, N., 2009. Nonlinear fluid–structure interaction calculation of the leakage behaviour of cracked concrete walls. Nuclear Engineering and Design, Volume 239, Issue 9 Pages 1628-1640. https://doi.org/10.1016/j.nucengdes.2008.09.001

Rastiello G., Leclaire S., Belarbi R., Bennacer R., 2015. Unstable two-phase flow rate in micro-channels and cracks under imposed pressure difference. International Journal of Multiphase Flow, Volume 77, Pages 131-141. https://doi.org/10.1016/j.ijmultiphaseflow.2015.08.009

Rastiello G., Tailhan JL., Rossi P., Del Pont S., 2015. Macroscopic probabilistic cracking approach for the numerical modelling of fluid leakage in concrete. Annals of Solid and Structural Mechanics, Volume 7, Pages 1–16. https://doi.org/10.1007/s12356-015-0038-6

Simon H., Nahas G., Coulon N., 2007. Air–steam leakage through cracks in concrete walls. Nuclear Engineering and Design, Volume 237, Issues 15–17, Pages 1786-1794. https://doi.org/10.1016/j.nucengdes.2007.03.025

Stegemann M., 2012. Large-scale experiments on the leakage behavior of cracked reinforced concrete walls. Germany: KIT Scientific Publishing

Sun, H.Q., Ding, J., Guo, J., Fu, D.L., 2011. Fractal Research on Cracks of Reinforced Concrete Beams with Different Aggregates Sizes. Advanced Materials Research, Volumes 250–253, Pages 1818–22. https://doi.org/10.4028/www.scientific.net/amr.250-253.1818.

Zemann, M., Herrmann, N., Dehn, F., 2019. Calcite formation on steamed concrete surfaces and its potential for sealing cracks. Construction and Building Materials, Volume 203, Pages 1-8. https://doi.org/10.1016/j.conbuildmat.2019.01.091

Zemann, M., Herrmann, N., Dehn, F., 2019. Leckageverhalten von gerissenem Beton – eine mehrskalige Betrachtung. [Leakage behavior of cracked concrete - A multiscale approach.] Beton- und Stahlbetonbau, Volume 114, Issue 12, Pages 929-937. https://doi.org/10.1002/best.201900057

Supplementary information

A – MACENA concrete formulation, preparation and quality control

The formulation of the MACENA project concrete is tabulated below with quantities given in kg/m^3 producing concrete with an overall density of 2343 kg/m^3 before drying.

Component	Dosage / kgm^{-3}
Cement CEM I 52,5 N CE CP2 NF Gaurain	320
Sand 0/4 REC GSM LGP1 Varennes	830
Gravel 4/11 R GSM LGP1 Varennes	445
Gravel 8/16 R Balloy	550
Sikaplast techno 80 (superplastifier)	2,6
Demineralised water *	195,53

* the free water is 167,89

The procedure for preparing the concrete is as follows:

1. The sand and gravel are dried at 80°C for 24 hours[7], stirring at least once during this time, and left to cool at least for another 24 hours before mixing. They can be stored in an airtight container after weighing.
2. The water is separated into two lots of a third ("absorbed water") and two thirds ("additional water").
3. The superplastifier is diluted in the added water.
4. The mixer is moistened with demineralised water.
5. The dry sand and gravel are placed in the mixer and the mixer is run for 1 minute.
6. The absorbed water is added and the mixer is run for 30 seconds.
7. The mixture is left to stand for 10 minutes if the mixer is watertight or 5 minutes if not.
8. The cement is added.
9. The mixer is started at the same time as a stopwatch is started.
10. After 1 minute has elapsed, the additional water is added.
11. After 5 minutes have elapsed the mixer is stopped.

Once the concrete has been poured into the mould, it is protected with cling film to limit the amount of water lost through evaporation. The concrete is left to harden for 20 hours before being removed from the mould and immersed in water for at least 28 days to cure.

The first batch of concrete was prepared in sufficient quantity to produce eight test cylinders for quality control in addition to casting the blocks for the main experiment. With this quantity of concrete it was possible to use a concrete mixer. For subsequent batches, the quantity of concrete was too small (2.5L) to use a mixer so it was mixed using the same procedure essentially but in a plastic bucket and stirred by hand.

Seven of the eight cylinders (11.25 cm diameter x 22.5cm long) were subjected to mechanical tests to determine the resistance to compression, Young's modulus and resistance to indirect tension ("Brazil test"). The results of the tests are summarised in the table below.

[7] On drying for 24 hours, the sand, Verennes gravel and Balloy gravel (which had been stored in a relatively dry state) lost 0.11%, 0.18% and 0.14% of their masses respectively.

Cylinder	Modulus / GPa	Resistance/ MPa	
		Compression	Indirect tension
1	-	45,07	-
2	35,54	46,76	-
3	35,14	46,58	-
4	35,84	46,91	-
5	-	-	4,02
6	-	-	4,70
7	-	-	4,20

The mean Young's modulus for cylinders 2-4 is 35,51 GPa (σ=0,35) and the mean resistance to compression for these cylinders is 46,75 MPa (σ=0,17). The mean resistance for cylinders 5-7 is 4,31 MPa (σ=0,35). It is notable that the resistance measured directly on cylinder 1 is slightly less than that measured on the cylinders 2-4, which had been subjected to cycles of compression up to 20 MPa during the measurement of the Young's Modulus before the resistance was measured.

The cylinders in the indirect tension tests all split neatly into two halves. Photographs of the fractured faces of half of each cylinder are show below. Most of the gravel grains through which the plane of the fracture passes have been split with only a few examples where the grain has remained virtually intact and most of these where the grain-cement boundary was close to the plane of the fracture.

Fractured faces of the cylinders after the indirect tension tests.

The 8th cylinder was used to measure the saturated density and porosity of the concrete. The weight of the water-saturated cylinder under water was 2976.2g and in air 5156.8g, giving a density of 2.365 g cm^{-3} (i.e. 0.94% more than theoretical density based on the formulation). The cylinder was dried at 80°C and weighed several times over the course of three days (graph below).

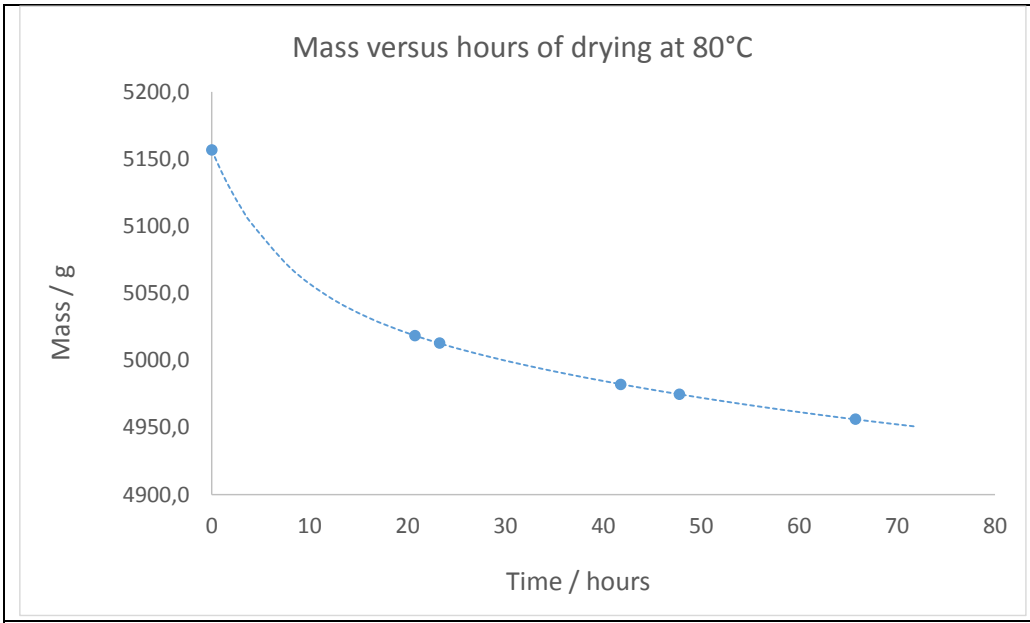

Mass of the cylinder versus hours of drying at 80°C with fitted double exponential trend.

The trend of the mass in g versus hours of drying was well fitted by a double exponential decay curve:

$$Mass = 4894{,}74 + 100{,}20\, e^{-0{,}1482t} + 161{,}86\, e^{-0{,}0148t}$$

in which the first term is the dry mass of the concrete, the second term represents water that is rapidly lost (free water or "macroporosity") and the third term represents water that is lost more slowly (absorbed water or "microporosity"). Taking the density of water as 1gcm^{-3} and supposing that the concrete of the cylinder was completely saturated with water at the beginning (i.e. there were no trapped air bubbles), the macroporosity accounts for 4.59% of the cylinder volume and the microporosity for 7.42% with a total porosity of 12.02%.

After drying for 66 hours, the resistance to compression of the 8th cylinder was measured while the cylinder was still hot as 41.9 MPa. Based on the above equation, the cylinder would have been 23.4% saturated.

B – Preparation of model cracks in concrete: moulds and assembly

In order to produce the concrete blocks with aluminium tubes and thermocouples embedded precisely, a pair of moulds were designed. The moulds were made from 5mm thick sheets of acrylic that were laser cut to allow them to slot together forming the basic block shape. By placing 3D printed plastic inserts at the bases of the moulds, model cracks with other profiles could be produced.

In the first design, the aluminium tubes were held in place by small discs of acrylic glued in place onto the base and the lid of the moulds. When the first blocks were cast, these circles became stuck inside the aluminium tubes and broke off. They were subsequently replaced by small round-head bolts which could be unscrewed from the base and the lid to aid removal. It was necessary to wrap the

heads of the bolts with aluminium tape to provide a snug fit for the aluminium tubes, which has the advantage of making it easier to dislodge the bolts from the tubes in the event that they become stuck. Holes were drilled in the lids so that the thermocouples could be passed through from above. These thermocouples were passed through a plastic coated foam rubber form 5mm thick stuck to the underside of the lid so as to leave a trench in the concrete where the thermocouples enter the concrete. This form was eventually removed and the trench was filled with a high-temperature epoxy potting compound (834ATH M. G. Chemicals) to ensure a good seal along the thermocouples and to protect the thermocouple wires. Pairs of holes drilled in the bases allowed the thermocouple junctions to be held in place by passing fishing line over them, clamping the small squares of mica (see explanation below) against the bases of the moulds in the process. Weights hung from the trailing ends of the fishing line provided the necessary tension to keep the thermocouples in place as the concrete was poured into the moulds. Small semicircles cut where the ends of the moulds touch the bases provided guides for a pair of semi-circular rods to leave grooves in the concrete where the rubber joints would be placed.

The main advantage of using acrylic sheet is its transparency, which makes the placement of the thermocouples and aluminium tubes a lot easier. A second advantage is that because the acrylic is slightly flexible, it is possible to remove the concrete from the mould by flexing the plastic to break the seal. The acrylic does not require a release agent and produces very smooth concrete surfaces with very few surface bubbles. A third advantage of acrylic is that it can be cleaned of concrete residues using strong hydrochloric acid, which restores the surface to its initial state. A fourth advantage of acrylic is that despite its inherent fragility, it can be repaired almost flawlessly using superglue producing a bond that is stronger than the acrylic itself.

The flexibility of the acrylic, however, presents the disadvantage that the mould can deform when the concrete is poured in, and support is required to prevent distortions in the resulting blocks. Initially the moulds were supported on a wooden frame which allowed the weights attached to the bases of the moulds to hang freely while providing somewhere to maintain the free ends of the thermocouple wires.

The first blocks prepared revealed a number of problems with the initial mould design:

1. In addition to the minor problem of the guides becoming stuck in the aluminium tubes (initially the lid was left in place while the concrete hardened) it turned out to be impossible to remove the lid without stripping the insulation off the thermocouples. Despite grease lubricating the holes in the lid through which the thermocouples were passed, the thermocouple insulation became caught on the acrylic[8]. It was therefore decided to cut the thermocouples cleanly with sufficient lengths of wire outside the concrete to allow them to be reconnected later rather than risk snapping the wires off too close to the concrete to be able to reconnect them. The holes in the mould lids were subsequently enlarged from 1mm to 2mm in order to provide greater clearance for the thermocouples. At the same time the holes in the bases of the moulds were enlarged from 0.5mm to 1mm to make it easier to thread the fishing line through the thermocouples.
2. Initially, polystyrene extrusions were used to create the grooves for the rubber joints but they were found to be too flexible and were quickly degraded by the concrete. They were

[8] The thermocouples becoming caught on the lid was one of the biggest problems encountered during sample preparation. Even with the holes enlarged there were still problems because the concrete was able to fill the holes around the thermocouples and prevent the lid from being removed without damaging the thermocouple or breaking the lid.

replaced with half-hardened copper extrusions, which held their shape better and were easier to reuse.

3. The first blocks produced suffered from a slight curvature along their lengths, which arose partly from a slight variation in the thickness of the acrylic but which was later found to be caused also by the weight of the concrete distorting the moulds. Steel supports were consequently added to the mould support frames to prevent the weight of the concrete deforming the sides of the moulds. Additionally, wooden braces could be placed over the moulds to prevent the sides from bulging outwards.

A photograph of the assembled moulds resting on the wooden supports just prior to filling with concrete is reproduced below. The free ends of the thermocouples are threaded onto the cross-bars to keep them out of the way. The weights hanging below are hidden by the steel supports, but the trailing ends of the threads from which the weights are hung can be seen.

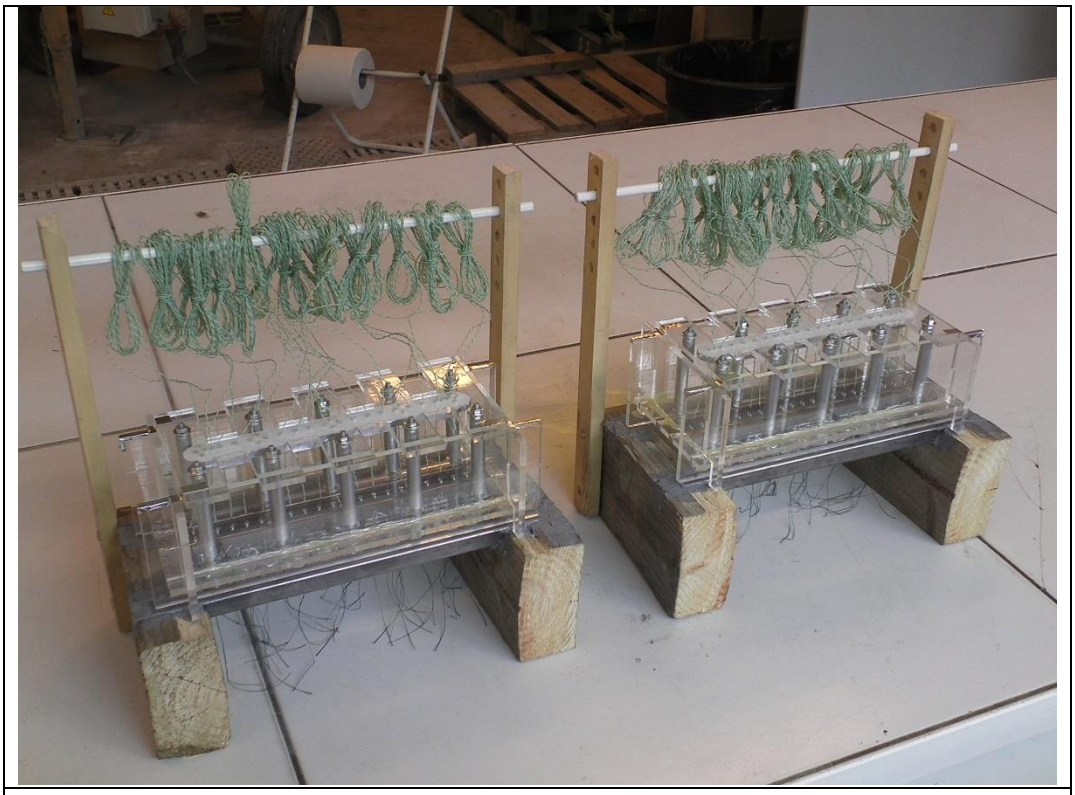

A pair of assembled moulds ready for concrete to be poured.

The reason for placing small squares of mica between the thermocouple junctions and the surfaces of the concrete blocks forming the inside of the model cracks was to reduce the tendency of the thermocouples to behave like cold fingers. The graph below shows the results of Castem[9] calculations of a model thermocouple embedded in a cylinder of concrete when the air above the cylinder is heated.

[9] http://www-cast3m.cea.fr

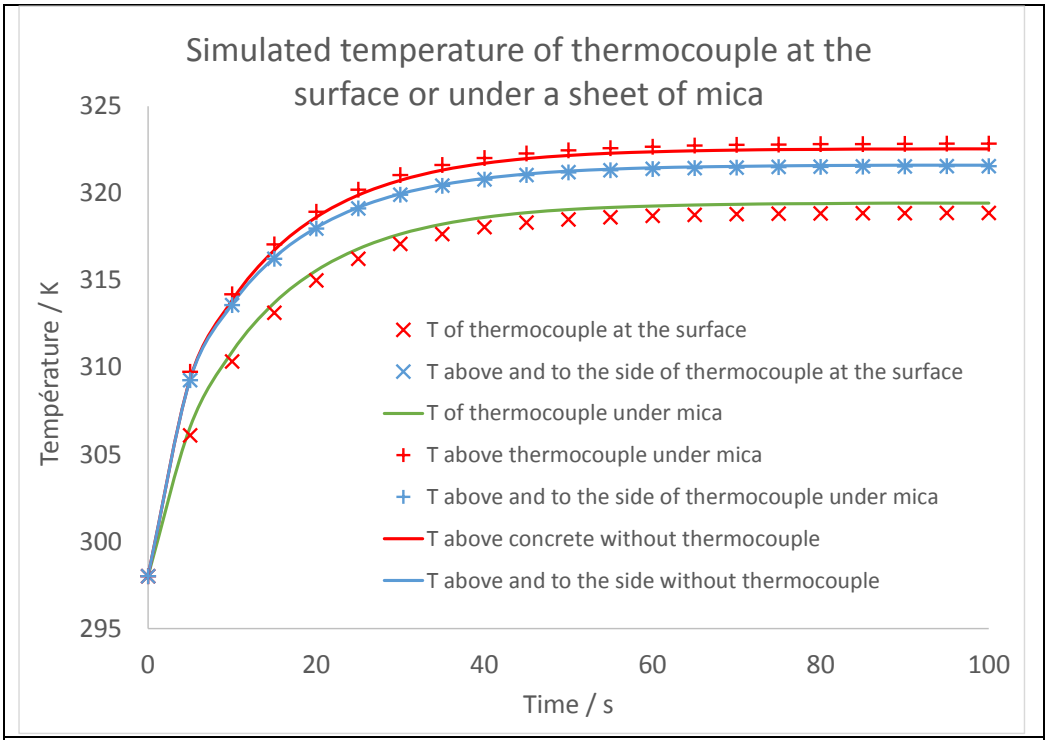

Results of Castem calculations to assess the effect on the temperature of placing thermocouples at the surface of the concrete or below a thin piece of mica.

When the thermocouple is at the surface of the concrete, i.e. when it makes contact with the air, the temperature of the thermocouple (red X) and the air in contact with it is several degrees lower than the surface of the concrete would be without the thermocouple (red line). When the thermocouple is below a thin sheet of mica, the temperature of the thermocouple (green line) is very close to that of the thermocouple at the surface, but the temperature of the surface of the mica and the air in contact with it (red +) is almost identical to the concrete without the thermocouple. The temperature at the surface slightly to the side of the thermocouple is practically the same in all three cases.

These calculations indicate that if the thermocouples, initially at ambient temperature, were to make direct contact with the heated mixtures of nitrogen and steam, they would almost certainly become the foci of condensation within the model crack. The sheet of mica slows the conduction of heat into the thermocouple from the air, thus preventing the thermocouple becoming a heat sink. Although the temperature of the thermocouple is slightly lower than the true temperature of the air inside the model crack as a result, the same temperature would be attained by a thermocouple at the surface because of the heat sink effect of the thermocouple.

The model cracks were formed by bolting the two blocks together with 1.6mm diameter rubber joints retained in grooves defining the sides of the crack. Steel spacers placed between the blocks could be used to ensure a minimum crack separation, and high-temperature silicone sealant ensured that the cracks were air-tight. It was found that treating the surfaces of the concrete to which the silicone was applied with epoxy resin improved the quality of the seal considerably, as otherwise the porosity of the concrete rendered the joint more porous. For the same reason, the faces of the assembled blocks with which the capsules made a seal also benefitted from being treated with epoxy resin.

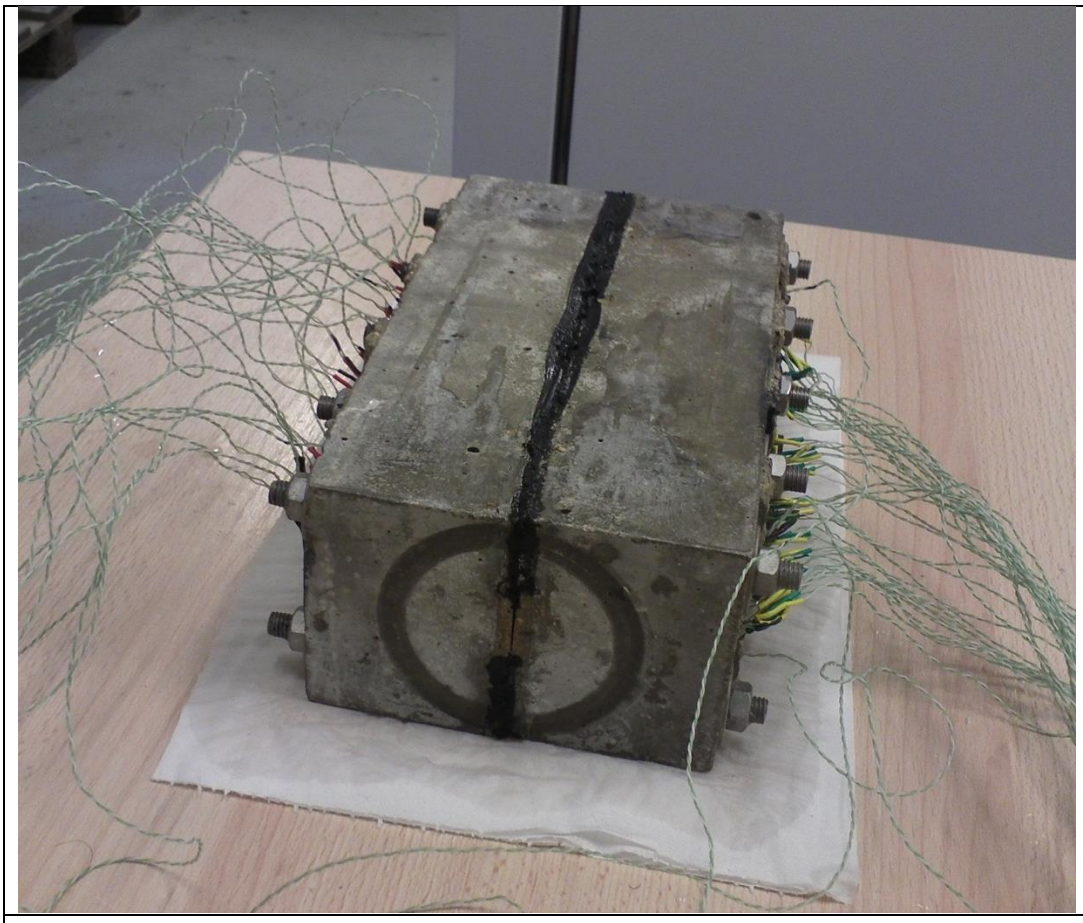

An assembled model crack.

The photograph above shows an assembled model crack. The circular mark indicates where the rubber joint of the capsules has made contact (this sample had already been the subject of some experiments). The thermocouples in this sample had to be cut in order to remove them from the mould without damaging them, and were later reconnected using solder and the heatshrink insulation is visible in the photo. The black smear between the blocks is the silicone sealant that was squeezed out when the blocks were assembled. By undoing the bolts and cutting this seal, it was possible to separate the blocks of assembled model cracks and use them to create a new model crack.

C – Pressure sensor calibration and additional temperature compensation

The pressure sensors were EFE model PHT861 with a 10 bar range compensated for temperatures in the range 20-175°C and an extended voltage range. The sensors were powered using a stabilised laboratory power supply set at 10.0 V. An initial test using the calibration parameters supplied by the manufacturer[10] revealed a discrepancy in the pressure sensor attached to the inlet capsule but the pressure sensor built into the nitrogen flow meter helped to identify which of the sensors required recalibration. An offset of 1.9018 mV was necessary to bring the inlet sensor into concordance with the outlet sensor; the measurements used for this calibration are reproduced in the graph below.

[10] The inlet sensor had a quoted zero signal of -0.0720 mV/V and sensitivity of 4.8150 mV/V and the outlet sensor had a quoted zero signal of -0.0100 mV/V and sensitivity of 4.8670 mV/V.

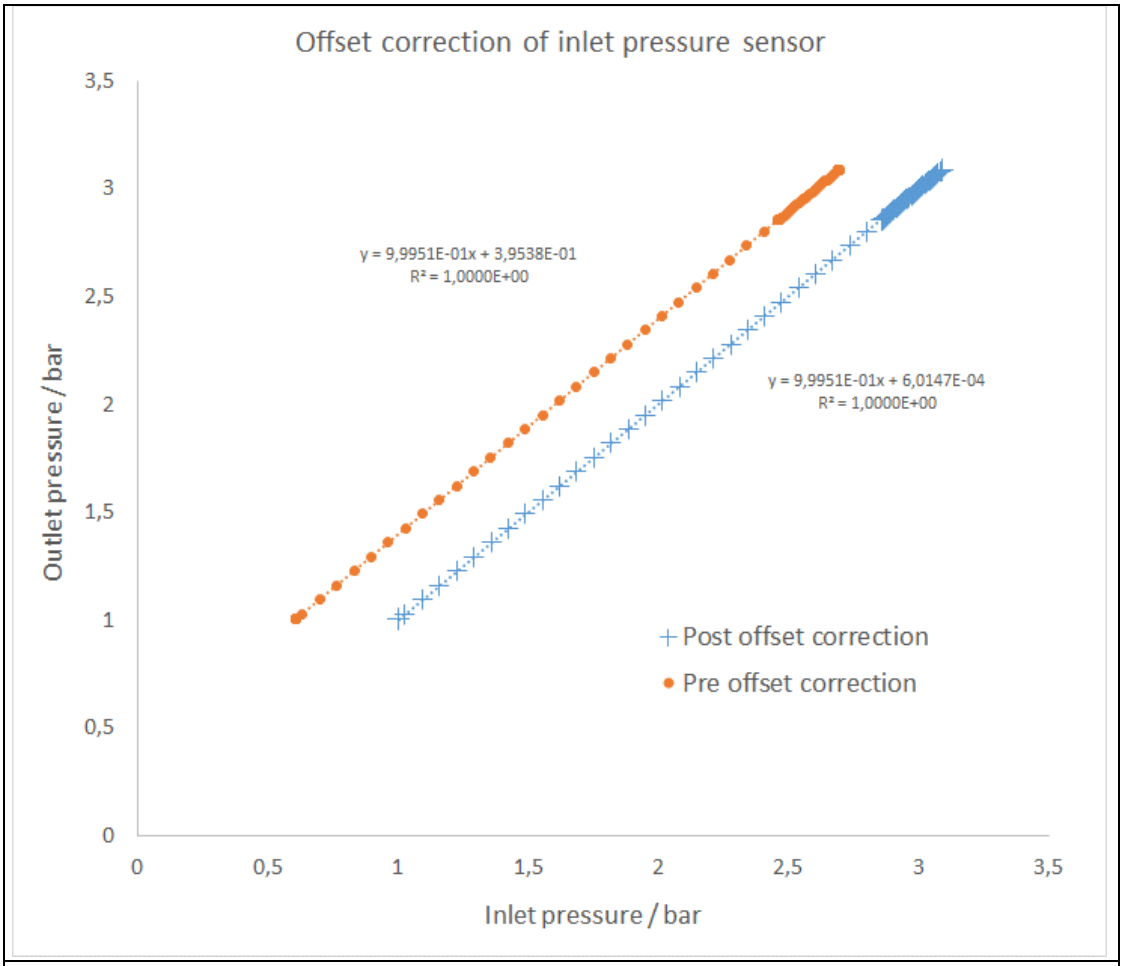

Data used to find the offset of the inlet pressure sensor.

Despite the temperature compensation incorporated in these pressure sensors, a noticeable variation in the measured pressure with changing temperature was found. By inserting an acrylic blanking plate with a large hole through the centre between the two capsules, a single airtight chamber was created and then heated. With the chamber open to the atmosphere the pressure was measured as the chamber cooled back down to room temperature. A plot of the measured pressure against the temperature of the sensor is given below. The gradients of the two trends were used to correct all of the pressure measurements to 25°C.

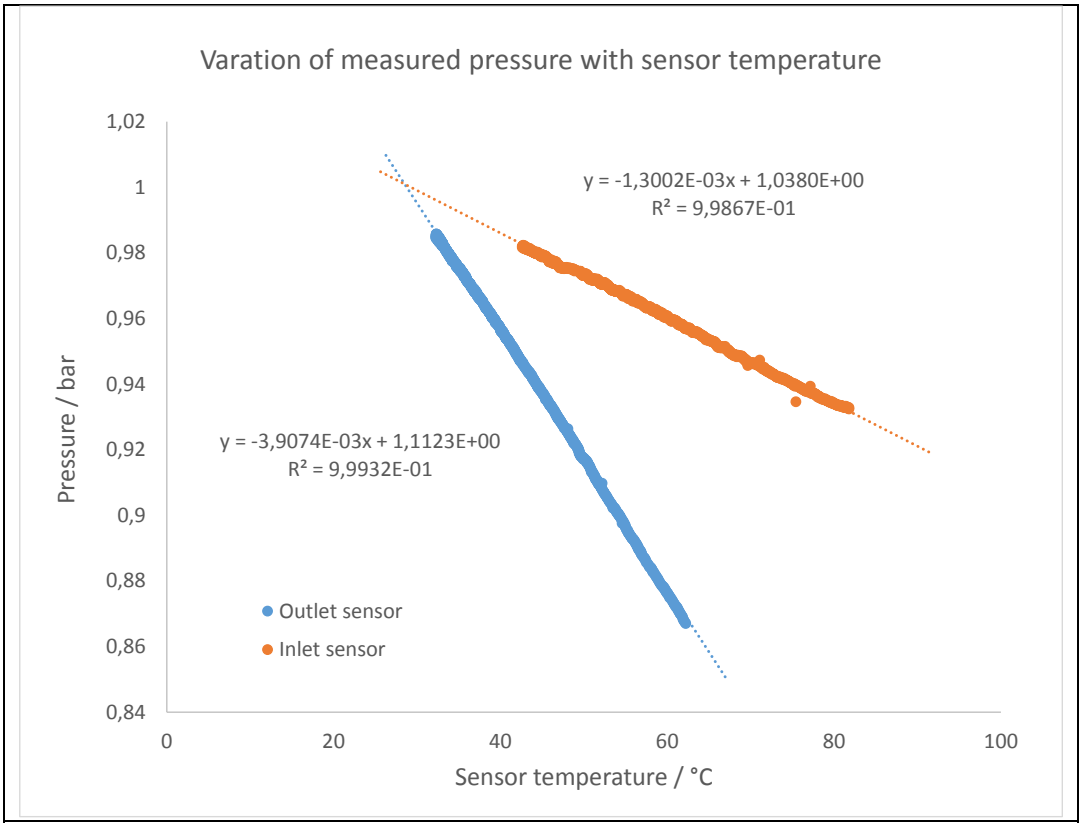

Results of an experiment to determine the temperature variation of the pressures measured by the sensors.

This calibration was stable for the initial series of experiments presented in this manuscript. However, for later experiments and experiments in which the concrete was pre-heated to 50°C the calibration was found to drift slightly. This phenomenon arose from the delay in the action of the self-correction/linearization mechanism of the pressure sensors, which requires minor changes to the calibration to ensure consistency between the sensor readings. These calibrations were accomplished using the same procedure as above to correct for differences of about 0.05 bar that otherwise arose between the sensor readings.

D – Magnetic field of the heating coil

The thermocouples and pressure sensors could be affected by the oscillating magnetic field of the heating coil when it is powered, producing errors of around 1°C. To minimise such interference the two halves of the heating element were coiled in opposite directions and mu-metal magnetic screens were placed between the coil and the sensors. The counter-coiling largely cancelled out the magnetic field in the region of the sensors, as confirmed by calculations using Castem (below) and the mu-metal sheet was able to screen the sensors from any residual field.

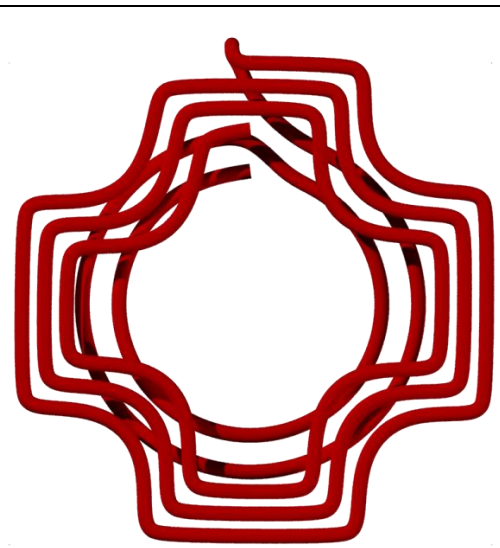

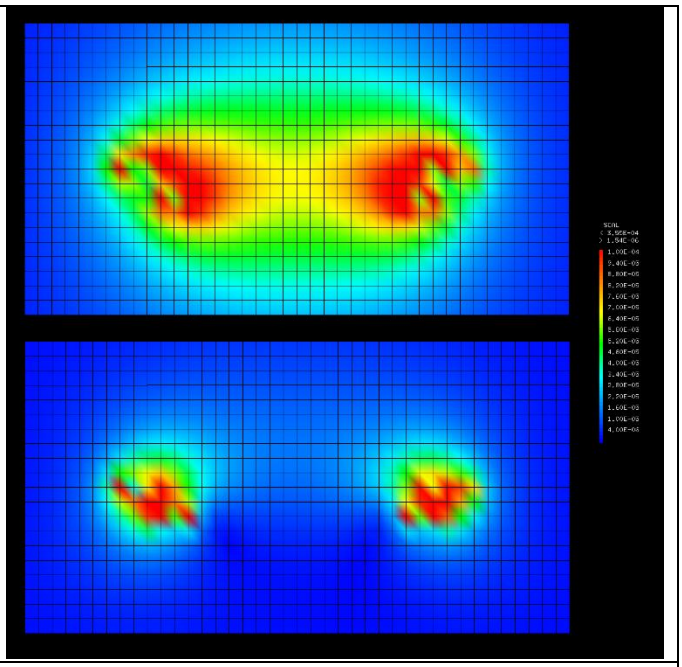

Design of the counter-coiled heating element and the magnetic fields through a horizontal slice calculated using Castem. In the calculation giving the upper results, the electric current in the circular part of the coil was reversed with respect to the other part in order to imitate the effect of it not being counter-coiled. In the calculation giving the lower results one can see that the counter-coiling significantly reduces the strength of the magnetic field at the centre of the coil, where the thermocouple and pressure sensor are placed.

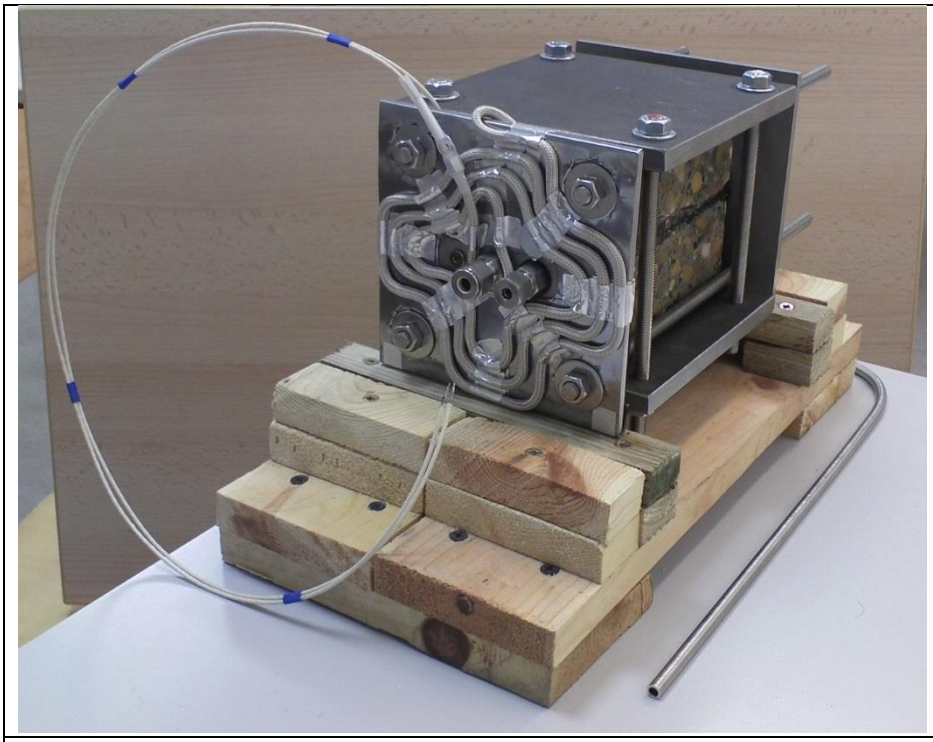

Assembled capsule with a test sample (this sample was held together with a press rather than embedded bolts) showing the heating coil and sheet of mu metal.

E – Calculating the effective crack separation

The derivation of the following equations is beyond the scope of this manuscript and is reported elsewhere. By incorporating an inertial term including fluid compressibility into the familiar equation for viscous flow between parallel plates, the pressure differential across a rectangular crack of length, l, width, w, and separation, h, can be expressed in terms of the volumetric flow rate, Q_v, as:

$$\Delta p = \frac{2p_o a' Q_v^2 + bQ_v}{1 - a' Q_v^2} \qquad a' = \frac{\rho_r}{2p_r}\frac{C}{h^4 w} l \qquad b = \frac{12\mu}{h^3 w} l$$

where p_o is the pressure at the crack outlet, p_r is a reference pressure when the fluid has the density ρ_r and μ is the dynamic viscosity. C is a dimensionless constant that depends on the crack properties that influence inertial losses (e.g. roughness and tortuosity). The mass flow rate, Q_m, is related to the volumetric flow rate through:

$$Q_m = Q_v \frac{p_i + p_o}{2p_r} \rho_r$$

where p_i is the pressure at the crack inlet.

If a series of nitrogen mass flow rates through a crack are set on the flow meter, waiting for the inlet and outlet pressures to stabilise after each adjustment, then a graph such as follows can be obtained.

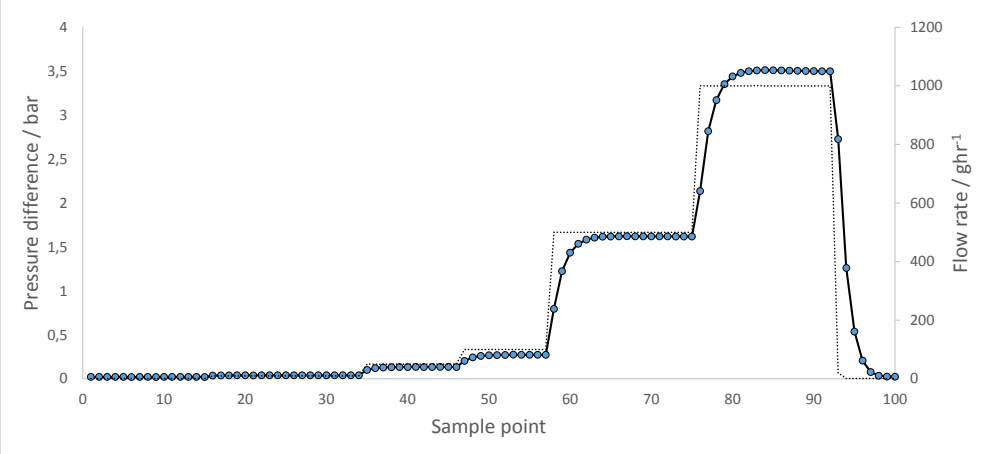

Each plateau from such a graph gives rise to a point relating the mass flow to the inlet and outlet pressures and their difference. Converting the mass flow rates to volumetric flow rates using the above relation, a second graph can be fitted to obtain values for the effective crack separation and the dimensionless constant, as below (the orange curve is the fitted relation and the blue points are the data points).

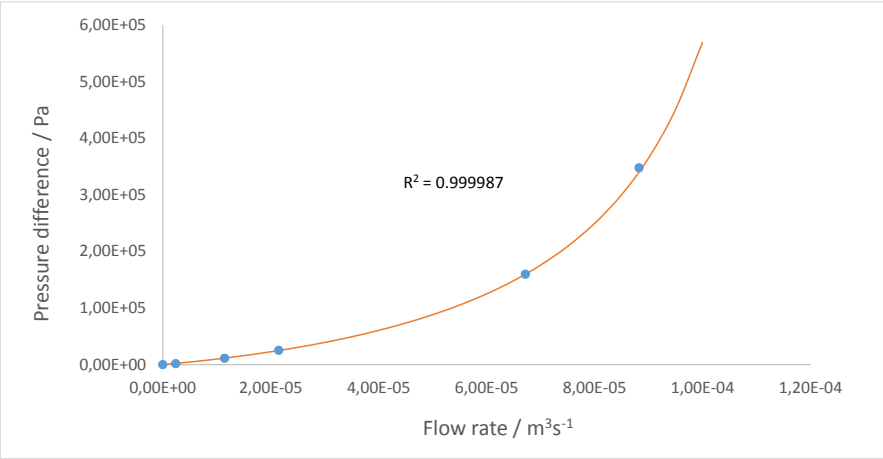

Provided that the flow regime is laminar, such experiments provide a very accurate value for the effective crack separation. In the example above, the final data point was excluded from the fit because the onset of non-laminar flow started to become important at this flow rate.

As well as using the limiting pressure differential values associated with a particular mass flow rate, it is also possible to write an equation for the inlet pressure with time:

$$\frac{dp_i}{dt} = \frac{RT}{m_r V}\left(Q_{m,in} - Q_v \frac{p_i + p_o}{2p_r}\rho_r\right)$$

where $Q_{m,in}$ is the incoming mass flow rate and the second term equates to the outgoing mass flow rate, m_r is the molar mass of the gas and V is the internal volume of the apparatus between the flow meter and crack opening. This equation does not lead to a simple integral, but it is trivial to solve iteratively using discrete time steps. The blue curve in the graph below is the iterative solution and the orange points the experimental values.

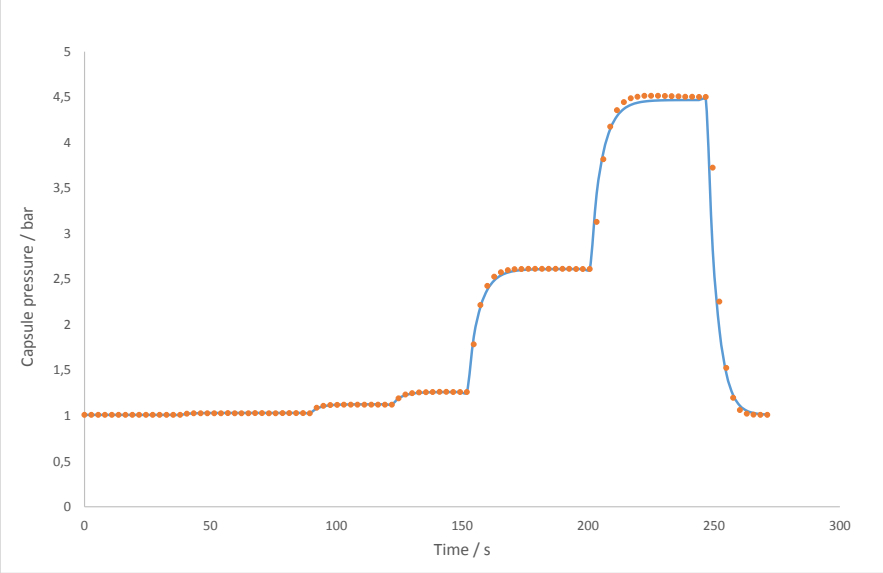

Similarly, it is possible to use such an iterative solution to fit the pressure drop curves obtained at the end of experiments. In the example plotted below, the experimental pressure values are shown with blue crosses and the orange line is the iterative solution obtained by fitting.

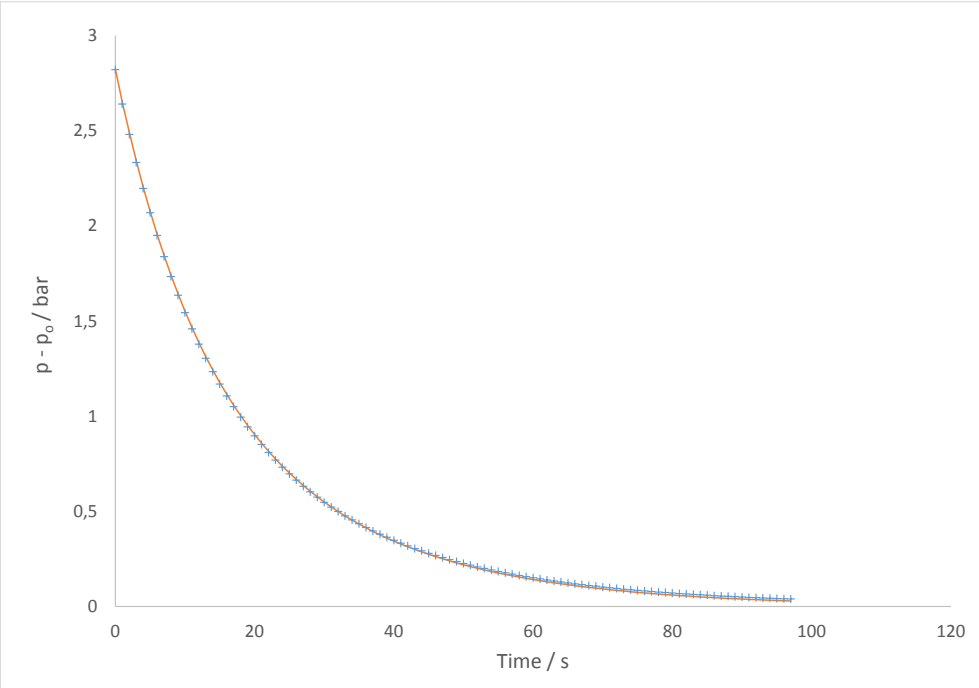

In this example, the crack separation obtained was 62.5 µm compared to 64.4 µm when fitting the pressure/flow rate curve for this crack. A drawback with fitting pressure drop curves is that they can be difficult to fit accurately if there is any interference at the time of the measurements, for example if the dropping pressure causes superheated water in the crack to boil, or in the case of more open cracks if the sampling rate is too low.

F – Ratios of theoretical limiting pressure

The above equations linking mass flow and pressure differential can be rearranged to calculate the theoretical limiting pressure for a given crack, non-condensing fluid mixture and temperature:

$$a\frac{2p_r}{\rho_r}Q_m^2 + b\frac{2p_r}{\rho_r}Q_m = \Delta p(\Delta p + 2p_o) \qquad a = \frac{C}{h^4 w}l \qquad b = \frac{12\mu}{h^3 w}l$$

Once the crack separation, h, and constant C have been obtained by fitting data from experiments with nitrogen at room temperature, it is possible to calculate theoretical values for the pressure differential at a given mass flow of any non-condensing steam/nitrogen mixture. Such a theoretical value implies that the concrete is at the same temperature as the fluid and, if steam is present, that the pressure does not rise above the vapour pressure of water at this temperature.

The ratios of theoretical and experimental values aid with the interpretation of experimental results for different crack separations by replacing the variations in flow rate and/or pressure with crack separation by a single value between 0 and 1.

It is also possible to take ratios between the theoretical values obtained for the nitrogen component of the mixtures at 20°C, and the theoretical values obtained for nitrogen/steam mixtures at 120°C, 140°C and 160°C. This produces the relationships shown below which are lower bounds to the experiments, since they are the pressures of the nitrogen cooled to the same temperature as the concrete and the volume of the condensed water neglected. The larger the crack separation or the

lower the total flow rate, the more linear the trend of the ratios against the proportion of steam in the mixtures.

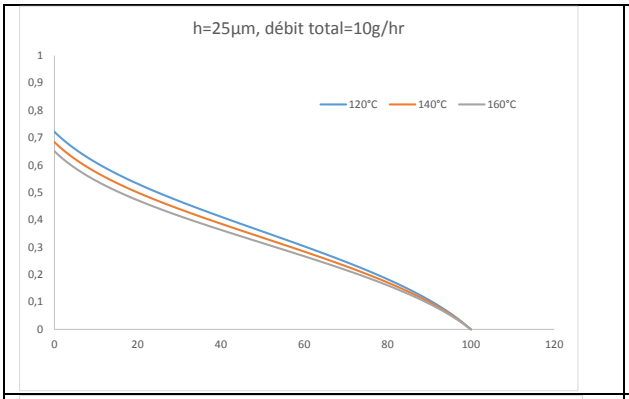

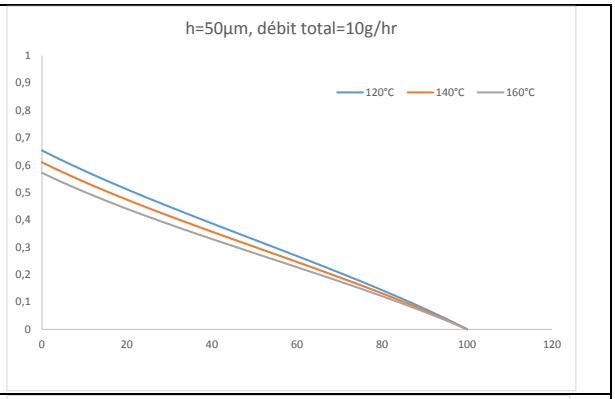

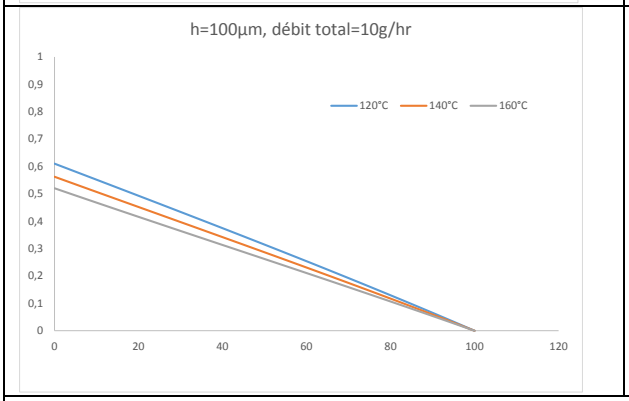

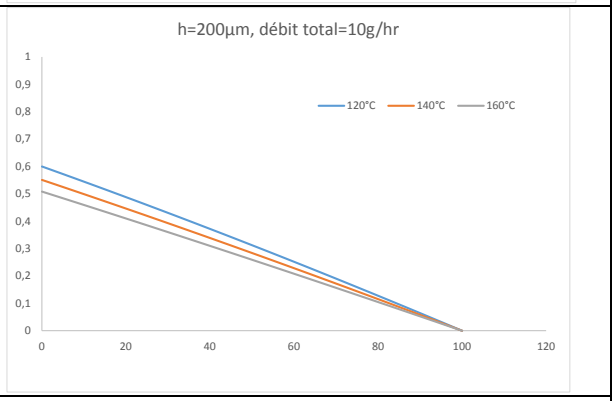

Ratios of theoretical limiting pressures for the nitrogen component at 20°C and steam/nitrogen mixtures at 120°C, 140°C and 160°C, plotted against the proportion of steam in the mixtures for a total flow rate of 10ghr^{-1}. From top left to bottom right, the crack separations are 25µm, 50µm, 100µm and 200µm.

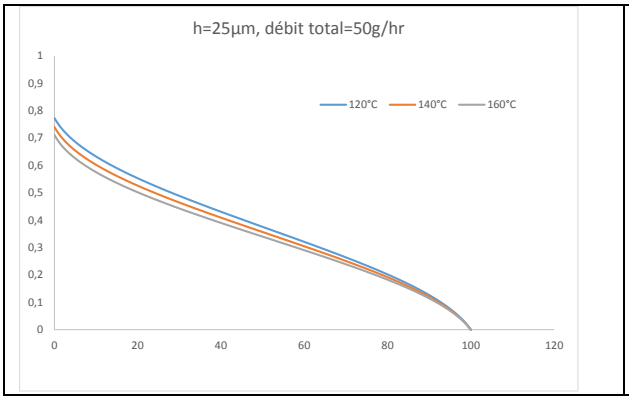

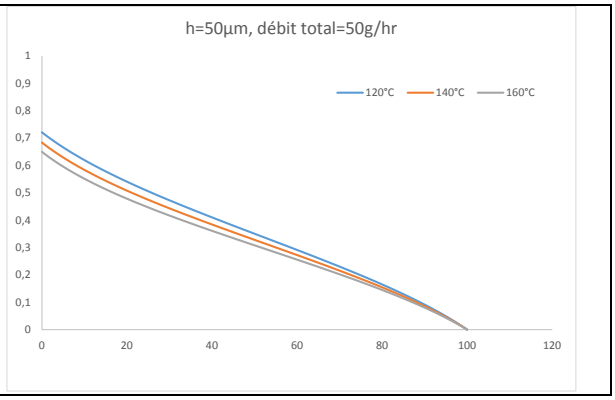

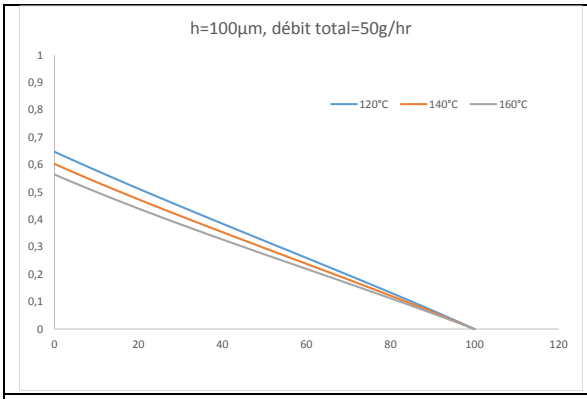

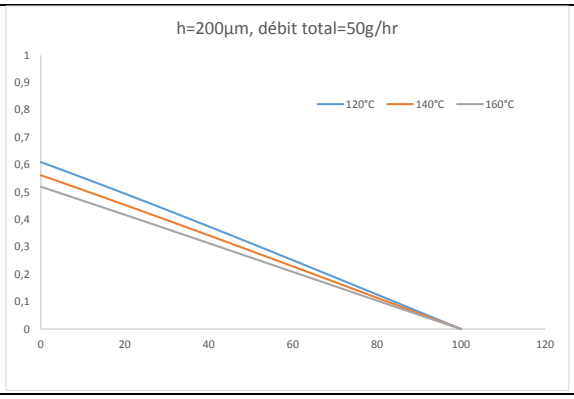

Ratios of theoretical limiting pressures for the nitrogen component at 20°C and steam/nitrogen mixtures at 120°C, 140°C and 160°C, plotted against the proportion of steam in the mixtures for a total flow rate of 50ghr^{-1}. From top left to bottom right, the crack separations are 25µm, 50µm, 100µm and 200µm.

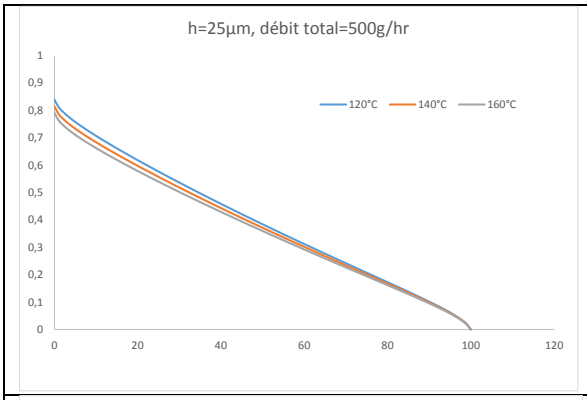

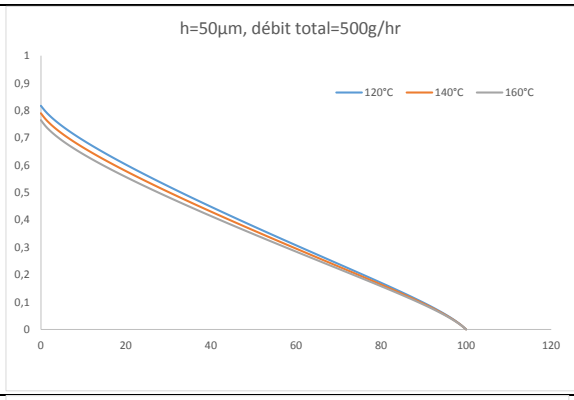

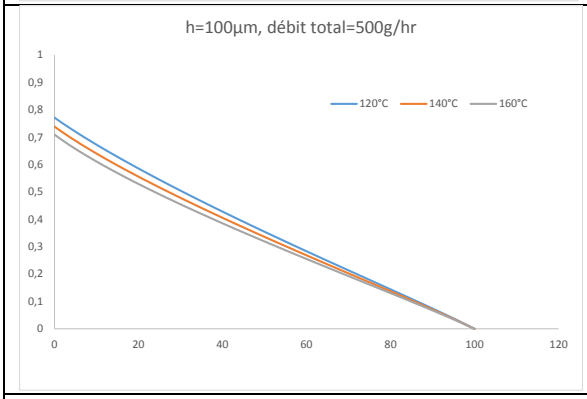

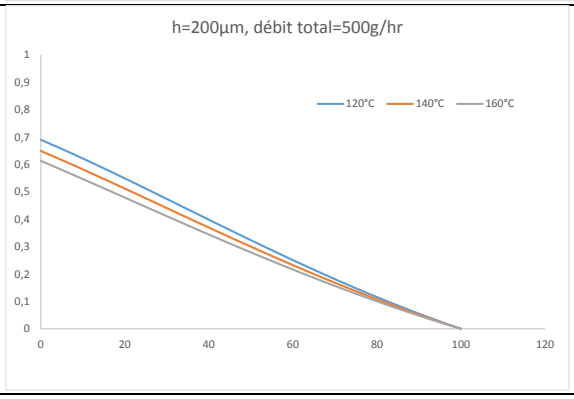

Ratios of theoretical limiting pressures for the nitrogen component at 20°C and steam/nitrogen mixtures at 120°C, 140°C and 160°C, plotted against the proportion of steam in the mixtures for a total flow rate of 500ghr^{-1}. From top left to bottom right, the crack separations are 25µm, 50µm, 100µm and 200µm.

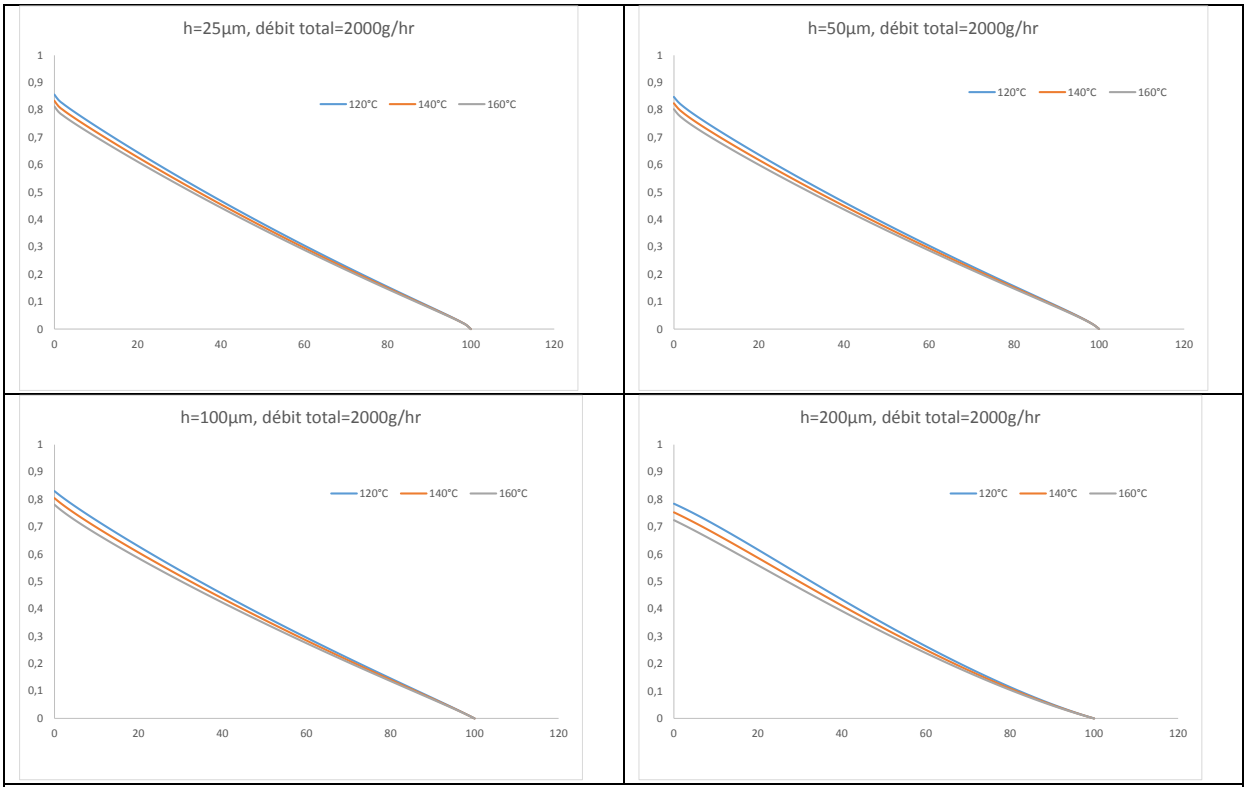

Ratios of theoretical limiting pressures for the nitrogen component at 20°C and steam/nitrogen mixtures at 120°C, 140°C and 160°C, plotted against the proportion of steam in the mixtures for a total flow rate of 2000ghr^{-1}. From top left to bottom right, the crack separations are 25µm, 50µm, 100µm and 200µm.